

PL-TR-95-2111

Environmental Research Papers, No. 1172

MODIFICATIONS TO THE REPRESENTATION OF THE SURFACE LAYER PROCESSES IN THE PHILLIPS LABORATORY GLOBAL SPECTRAL MODEL

**Chien-Hsiung Yang
Douglas C. Hahn
Sam S. Chang
Donald L. Aiken**

8 AUGUST 1995

APPROVED FOR PUBLIC RELEASE; DISTRIBUTION UNLIMITED.



**PHILLIPS LABORATORY
Directorate of Geophysics
AIR FORCE MATERIEL COMMAND
HANSCOM AIR FORCE BASE, MA 01731-3010**

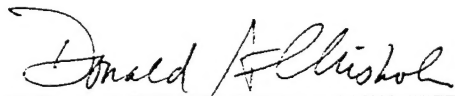
19960715 074

DISCLAIMER NOTICE

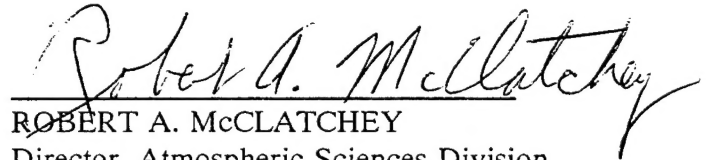


THIS DOCUMENT IS BEST QUALITY AVAILABLE. THE COPY FURNISHED TO DTIC CONTAINED A SIGNIFICANT NUMBER OF PAGES WHICH DO NOT REPRODUCE LEGIBLY.

This technical report has been reviewed and is approved for publication.



DONALD A. CHISHOLM , Chief
Satellite Analysis and Weather
Prediction Branch



ROBERT A. McCLATCHEY
Director, Atmospheric Sciences Division

This document has been reviewed by the ESC Public Affairs Office (PA) and is releasable to the National Technical Information Service (NTIS).

Qualified requestors may obtain additional copies from the Defense Technical Information Center (DTIC). All others should apply to the NTIS.

If your address has changed, if you wish to be removed from the mailing list, or if the addressee is no longer employed by your organization, please notify PL/TSI, 29 Randolph Road, Hanscom AFB, MA 01731-3010. This will assist us in maintaining a current mailing list.

REPORT DOCUMENTATION PAGE			Form Approved OMB No. 0704-0188	
Public reporting burden for this collection of information is estimated to average 1 hour per response, including the time for reviewing instructions, searching existing data sources, gathering and maintaining the data needed, and completing and reviewing the collection of information. Send comments regarding this burden estimate or any other aspect of this collection of information, including suggestions for reducing this burden, to Washington Headquarters Services, Directorate for Information Operations and Reports, 1215 Jefferson Davis Highway, Suite 1204, Arlington, VA 22202-4302, and to the Office of Management and Budget, Paperwork Reduction Project (0704-0188), Washington, DC 20503.				
1. AGENCY USE ONLY (Leave blank)		2. REPORT DATE August 1995		3. REPORT TYPE AND DATES COVERED Final Report
4. TITLE AND SUBTITLE Modifications to the Representation of the Surface Layer Processes in the Phillips Laboratory Global Spectral Model			5. FUNDING NUMBERS PE 61102F PR 2310 TA CP WU 13	
6. AUTHOR(S) Yang, Chien-Hsiung Chang, Sam S.			Hahn, Douglas C. Aiken, Donald L.	
7. PERFORMING ORGANIZATION NAME(S) AND ADDRESS(ES) Phillips Laboratory (GPAB) 29 Randolph Road Hanscom Air Force Base, Massachusetts 01731-3010			8. PERFORMING ORGANIZATION REPORT NUMBER PL-TR-95-2111 ERP, No. 1172	
9. SPONSORING/MONITORING AGENCY NAME(S) AND ADDRESS(ES)			10. SPONSORING/MONITORING AGENCY REPORT NUMBER	
11. SUPPLEMENTARY NOTES				
12a. DISTRIBUTION / AVAILABILITY STATEMENT Approved for public release; distribution unlimited			12b. DISTRIBUTION CODE	
13. ABSTRACT (Maximum 200 words) This report documents the recommended modifications to the ways by which surface-layer processes have been represented in the Phillips Laboratory Global Spectral Model (PL-GSM). Firstly, new formulas for surface-layer exchange coefficients and a new method of defining roughness lengths over water replace the earlier version. Secondly, the scope of surface energy balance is expanded to include latent energy of phase transformation of water at the surface. The logic and order of executing the corresponding numerical procedure is accordingly modified. A number of other minor changes in either definition or computation that are found desirable or necessary are also made. The report consists of two parts. It starts with a description of the recommended changes element by element that includes isolated analysis of the individual changes. It then presents analyses of static comparisons of the outputs from various versions of the representation and concludes with the final recommendation.				
14. SUBJECT TERMS Boundary layer parameterization Exchange coefficients			15. NUMBER OF PAGES 16. PRICE CODE	
17. SECURITY CLASSIFICATION OF REPORT Unclassified			18. SECURITY CLASSIFICATION OF THIS PAGE Unclassified	
19. SECURITY CLASSIFICATION OF ABSTRACT Unclassified			20. LIMITATION OF ABSTRACT SAR	

Contents

1.	INTRODUCTION	1
2.	FORMAL CHANGES	3
2.1	Surface Layer Exchange Coefficients	4
2.2	Roughness Lengths Over Oceans	8
3.	STRUCTURAL CHANGES	16
3.1	Parametric Representation of Surface Energy Fluxes	16
3.2	Solving the Surface Energy Balance Equation	19
3.3	Monteith's Psychrometer Constant	23
3.4	Definition of Plant Coefficient	25
3.5	Types of Precipitation at the Surface	25
3.6	Boundary Conditions for the Evolution of Soil Temperature	27
4.	EXPERIMENTS	28
4.1	Plant Coefficient	33
4.2	Exchange-Coefficient Formulas and Energy-Balance Algorithm	38
4.3	Methods of Solving Energy-Balance Equations	60
5.	SUMMARY AND CONCLUSIONS	66
	REFERENCES	69

Illustrations

1.	Roughness Length for Momentum, z_{0M} , as Solutions of the Charnock Equation for Different Values of the Charnock Constant, vs the Wind Speed V at 40 m Above Surface.	10
2.	Friction Velocity, u_* Corresponding to z_{0M} of Fig. 1, vs the Wind Velocity V at 40 m Above Surface.	10
3.	Roughness Lengths z_{0m} for Momentum, z_{0q} for Water Vapor, and z_{0t} for Heat vs Wind Speed V at 40 m Above Surface. (a) $2 \geq V > 0$, in m/s, (b) $25 \geq V \geq 1$, in m/s.	12
4.	Roughness Lengths for Momentum, z_{0M} . A: ECMWF. B: PL-91. (a) $2 \geq V > 0$, in m/s, (b) $25 \geq V \geq 1$, in m/s.	13
5.	Ratio of Roughness Lengths, z_{0q}/z_{0m} and z_{0t}/z_{0m} According to the ECMWF Formulas.	14
6.	Ratios of the New to Old Exchange Coefficients: RCM for Momentum, RCH for Heat, and RCQ for Water Vapor. (a) $2 \geq V > 0$, in m/s, (b) $25 \geq V \geq 1$, in m/s.	15
7.	A Map of Model Gridpoints in the Region of Study, Southeastern United States. Each Gridpoint is Associated With Three Indices of Land Specification.	29

8.	A Series of Weather Maps Over the United States During the Period of Study, Jan. 12, 12 UTC - Jan. 15, 12 UTC, 1979.	31
9A.	Pairwise Comparisons of Surface Temperatures Between the Old and New Exchange Coefficients at Gridpoints (2,2) and (2,4).	49
9B.	Same as in Figure 9A, Except for Gridpoints (7,2) and (7,4)	50
10A.	Pairwise Comparisons of Sensible Heat Fluxes Between the Old and New Exchange Coefficients at Gridpoints (2,2) and (2,4).	51
10B.	Same as in Figure 10A, Except for Gridpoints (7,2) and (7,4).	52
11A.	Pairwise Comparisons of Surface Temperatures Between the Old and New Algorithms at Gridpoints (2,2) and (2,4).	53
11B.	Same as in Figure 11A, Except for Gridpoints (7,2) and (7,4).	54
12A.	Pairwise Comparisons of Sensible Heat Fluxes Between the Old and New Algorithms at Gridpoints (2,2) and (2,4)	55
12B.	Same as in Figure 12A, Except for Gridpoints (7,2) and (7,4).	56
13.	Comparisons of Sensible Heat Fluxes Between the Old (A1) and New (B2) Models at Gridpoints (2,2), (2,4), (7,2), and (7,4)	61
14.	Comparisons of Evaporative Latent Heat Fluxes Between the Old (A1) and New (B2) Models at Gridpoints (2,2), (2,4), (7,2), and (7,4).	62

Tables

1.	The Ratio of $(N_2)_{\text{new}}$ to $(N_2)_{\text{old}}$	7
2.	The Ratio of $(F_2)_{\text{new}}$ to $(F_2)_{\text{old}}$	7
3.	The Ratio of $(ch)_{\text{new}}$ to $(ch)_{\text{old}}$	7
4.	The Old and New Classifications of Precipitation at the Surface.	26
5.	A Comparison of Surface Outputs Between the Old (UG-91) and New Plant-Coefficient Formulations With the Old Exchange Coefficients, at Timestep = 1.	34
6.	Same as in Table 5, Except for Timestep = 19.	35
7.	A Comparison of Surface Outputs Between the Old (UG-91) and New Plant-Coefficient Formulations With the New Exchange Coefficients, at Timestep = 1.	36
8.	Same as in Table 7, Except for Timestep = 19.	37
9.	A Schematic Diagram of Impact Evaluation.	38
10a.	Summary Tables of Statistics of Models A1, A2, B1, and B2 at Gridpoint (2,2) for Variables t1 and q1.	40

10b.	Same as in Table 10a, Except for Variables H and E.	41
11a.	Same as in Table 10a, Except for Gridpoint (2,4).	42
11b.	Same as in Table 10b, Except for Gridpoint (2,4).	43
12a.	Same as in Table 10a, Except for Gridpoint (7,2).	44
12b.	Same as in Table 10b, Except for Gridpoint (7,2).	45
13a.	Same as in Table 10a, Except for Gridpoint (7,4).	46
13b.	Same as in Table 10b, Except for Gridpoint (7,4).	47
14.	A Comparison of Surface Energy Fluxes Obtained with Different Methods of Solving the Surface Energy Balance, at Gridpoint (2,2).	64
15.	Same as in Table 14, Except for Gridpoint (7,4).	65

Acknowledgement

We thank Mr. Donald A. Chisholm for his unfailing support and continual encouragement without which this report would not have seen the light of day. Our special gratitude is due Mrs. Audrey Campana for her boundless patience and unflinching attention to details while preparing the manuscript.

Modifications to the Representation of the Surface Layer Processes in The Phillips Laboratory Global Spectral Model

1. INTRODUCTION

The topic, representation of surface-layer processes in the dynamics of the atmosphere, is embodied as a part of the Phillips Laboratory Boundary Layer System (PL-BLS) which is in turn a component in the Phillips Laboratory Global Spectral Model (PL-GSM).

PL-GSM is a global model of the dynamics of the atmosphere designed for medium-range weather forecasts. It may be conveniently described as a spectral primitive-equation model of the moist atmosphere in which three physical processes: radiative transfer, sub-grid scale convections, and interactions with the solid earth, are represented individually at gridpoints and connected serially, parameterized in terms of variables and parameters defined on the grid scale. A series of technical reports is available^{1,2,3,4} for information on the model.

The component of PL-GSM that represents the physics of interactions between the atmosphere and the solid earth is called the Phillips Laboratory Boundary Layer System (PL-BLS). It is a product of joint efforts between the scientists of the Laboratory and the associates and students of Professor Larry Mahrt of the Oregon State University (OSU). It applies OSU's so-called coupled-atmosphere-plant-soil (CAPS) model at each land gridpoint, which is specified with values of a set of characteristic parameters required by the model. The initial design of CAPS is described in Mahrt et al. (1984),⁵ while a later version on which this report is based is presented in Mahrt et al. (1987).⁶ The methodology for devising the global land surface specification employed in this study will be documented in a separate report. At gridpoints that are over water, the current practice specifies surface temperature with the climatological values and assumes saturation at that temperature for the corresponding surface specific humidity.

CAPS models the physics of interaction between the atmosphere and the solid earth in three layers: one transitional layer in the air, commonly referred to as the turbulent mixing layer; another transitional layer in the soil of a limited depth immediately beneath the surface, and the third, which separates the first two, is an air layer adjacent to the surface and is called the surface layer. The turbulent mixing and surface layers together make up the so-called planetary boundary layer (PBL). Within each of the transitional layers, the dynamics of the state variables are, in addition to being influenced by body as well as inertia forces, subjected to diffusion in which diffusivity is characteristic of the state of the medium. Both transitional layers are divided into a number of sublayers (for example, two-layer soil Thermodynamic Model) for discretization in practice. In the surface layer, which may be viewed as a buffer and a coupling that maintains an equilibrium at any moment, various fluxes are assumed constant within the layer and are determined by boundary values and layer conductances. These momentum and energy fluxes determine the rates of exchanges between the atmosphere and the solid earth.

Until recently, that is, up to the 1992 version of PL-GSM, we have used the formulas and values for boundary layer parameters that were recommended to us by

the OSU group previously and adopted almost verbatim the entire numerical procedure of CAPS. In 1991, the OSU group substantially revised⁷ the formulas for surface-layer exchange coefficients and, in 1994, introduced us⁸ to the method of estimating roughness lengths over oceans suggested by a group of scientists⁹ at the European Centre for Medium Range Forecasts (ECMWF). It soon became obvious as we started responding to these revisions that a systematic and in-depth review of the representation of surface-layer processes in CAPS should accompany any effort to install these or other potential changes. The review led to modifications in the ways some surface-layer phenomena are modeled and in the manner surface energy balance is sought. This report discusses these modifications and documents the changes introduced.

For convenience, we shall classify changes into two kinds and discuss them separately. Changes in formulas and methods of estimation, as recommended by the OSU group, are referred to as the formal change while changes in modeling or procedures are called the structural change. Section 2 treats the former and Section 3 the latter. Section 4 presents the setting and the method we used to assess the impacts of different changes on results of the representation. Section 5 presents the conclusions.

Throughout the rest of the report, we shall use as the standard reference the "OSU 1-D PBL Model User's Guide," version 1.0.4 by M. Ek and L. Mahrt of the Department of Atmospheric Sciences, Strand Agriculture Hall, Room 326, Oregon State University, Corvallis, OR 97331-2209, U.S.A., prepared March 1991. It will be referred to simply as the 91 User's Guide and designated as UG-91. Terms used and formulas employed will be kept aligned as closely as possible to the usage in the UG-91.

2. FORMAL CHANGES

Two formal changes are considered. One is in the formulas for surface-layer exchange coefficients and the second is in the method of estimating roughness lengths over oceans. Here, the changes refer to the differences between those employed in the

1992 PL-GSM (referred to as the 'old') and those in the latest recommendations (called the 'new').

2.1 Surface Layer Exchange Coefficients

(a) When $|\mathbf{v}_2| > 0$, where \mathbf{v}_2 is the horizontal wind at the top of the surface layer, exchange coefficients, cm for momentum and ch for heat may be put in the forms, respectively,

$$cm = N_1 F_1, \text{ and } ch = N_2 F_2, \quad (1)$$

where the N 's and F 's represent the factors that are, respectively, independent of and functions of, the static stability of the layer. In the new version, these factors are given, respectively, by

$$N_1 = \left(\frac{k}{\ln \frac{z_2}{z_{0M}}} \right)^2 |\mathbf{v}_2|, \quad N_2 = \frac{1}{R} \left(\frac{k^2}{\ln \frac{z_2}{z_{0M}} \ln \frac{z_2}{z_{0H}}} \right) |\mathbf{v}_2|, \quad (2)$$

$$F_1 = \begin{cases} e^{-Ri_B}, & \text{if } Ri_B > 0 \\ 1 - \frac{b_1 Ri_B}{1 + c_1 \frac{k^2}{\left(\ln \frac{z_2}{z_{0M}} \right)^2} \left(Ri_B \frac{z_2}{z_{0M}} \right)^{1/2}}, & \text{if } Ri_B < 0 \end{cases} \quad (3)$$

$$F_2 = \begin{cases} e^{-Ri_B}, & \text{if } Ri_B > 0 \\ 1 - \frac{b_2 Ri_B}{1 + c_2 \frac{k^2}{\ln \left(\frac{z_2}{z_{0M}} \right) \ln \left(\frac{z_2}{z_{0H}} \right)} \left(Ri_B \frac{z_2}{z_{0H}} \right)^{1/2}}, & \text{if } Ri_B < 0 \end{cases} \quad (4)$$

Here, \mathbf{v}_2 and z_2 are the horizontal wind in meters per second and the height above ground in meters at the top of the surface layer, $k = 0.4$ is the von Karman constant, and $R = 1.0$ is the ratio of the drag coefficient for momentum to that for heat (after Ref. 7). Parameters b 's and c 's are universal constants with the following values:

$$b_1 = 10, c_1 = 75, b_2 = 15, c_2 = 75. \quad (5)$$

z_{0M} and z_{0H} are roughness length for momentum and for heat, respectively. PL-GSM has had a set of fixed values of z_{0M} for each of the Gaussian gridpoints derived from a source at the U.S. National Centers for Environmental Prediction (NCEP). Currently z_{0H} is set at a hundredth of z_{0M} following the conventional wisdom. Ri_B is the bulk Richardson number for the layer and is defined as

$$Ri_B = \frac{g z_2 (\theta_{v1} - \theta_{v2})}{\theta_{v1} |\mathbf{v}_2|^2} \quad (6)$$

in which $\theta_{v1} = \theta_1 (1 + 0.61 \times q_1)$ and $\theta_{v2} = \theta_2 (1 + 0.61 \times q_2)$ are the virtual potential temperatures, respectively, at the surface and at the top of the surface layer. The q 's denote specific humidity,

The old exchange coefficients are also defined by Eqs. (1) - (6) but with different specifications of the parameters as listed below:

$$\begin{aligned} z_{0H} &= z_{0M} \\ R &= 0.74 \end{aligned} \quad (7)$$

$$b_1 = 9.4, c_1 = 69.56, b_2 = 9.4, c_2 = 49.80$$

(b) When $|\mathbf{v}_2| = 0$, the new formulas set

$$cm = \begin{cases} 1 \times 10^{-6}, & \text{if } \theta_{v2} \geq \theta_{v1} \\ \frac{2}{15} \left(\frac{g z_2 (\theta_{v1} - \theta_{v2})}{\theta_{v1} z_2 / z_{0M}} \right)^{1/2}, & \text{if } \theta_{v2} < \theta_{v1} \end{cases} \quad (8)$$

$$ch = \begin{cases} 1 \times 10^{-6}, & \text{if } \theta_{v2} \geq \theta_{v1} \\ \frac{1}{5} \left(\frac{g z_2 (\theta_{v1} - \theta_{v2})}{\theta_{v1} z_2 / z_{0H}} \right)^{1/2}, & \text{if } \theta_{v2} < \theta_{v1} \end{cases} \quad (9)$$

and

$$Ri_B = 1 \times 10^3 \quad (10)$$

In contrast, the old has

$$cm = \begin{cases} 1 \times 10^{-300}, & \text{if } \theta_{v2} \geq \theta_{v1} \\ \frac{1}{7.4} \left(\frac{g z_2 (\theta_{v1} - \theta_{v2})}{\theta_{v1} z_2 / z_{0M}} \right)^{1/2}, & \text{if } \theta_{v2} < \theta_{v1} \end{cases} \quad (11)$$

$$ch = \begin{cases} 1 \times 10^{-300}, & \text{if } \theta_{v2} \geq \theta_{v1} \\ \frac{cm}{.716}, & \text{if } \theta_{v2} < \theta_{v1} \end{cases} \quad (12)$$

and

$$Ri_B = 1 \times 10^5 \quad (13)$$

It is remarked here that in CAPS the conductance of air for water vapor is assumed the same as that for heat, be it expressed by exchange coefficient as here or by diffusivity in the turbulent mixing layer. It is also noted that the present usage of subscripts deviates from that practiced in UG-91: specifically, the numerical subscripts 1 and 2 designate the bottom, that is, the surface, and the top, respectively, of the surface layer, while any alphabetical suffix is regarded as a part of the variable name to which it is affixed.

When $|\mathbf{v}_2| \neq 0$, the change is threefold: a new value for R , the ratio of drag coefficient for momentum to that for heat, the introduction of z_{0H} , roughness length for heat, distinct from z_{0M} , and a different set of values for constant parameters in the

stability-dependent factor F 's. The effect on cm comes only from the third change and appears only when the layer is unstable. With any likely value of z_{0H} being smaller than that of z_{0M} , the change in cm is significantly smaller than the corresponding change in ch .

The most obvious of the changes in ch is a reduction by a factor of 0.74 due to the larger value for R irrespective of the layer stability. The other stability-independent reduction arises from the fact that the current conventional wisdom says z_{0H} is anything but equal to or greater than z_{0M} (see, for example, Holtslag, A.A.M. and Beljaars, A.C.M. (1988)¹⁰.

Tables 1 - 3, prepared using the ratio $z_2/z_{0M} = 50$, illustrate the impacts from each factor as well as the total effect.

Table 1. $(N_2)_{\text{new}}/(N_2)_{\text{old}}$

$(N_2)_{\text{new}}/(N_2)_{\text{old}}$	z_{0H}/z_{0M}		
	0.1	0.01	0.001
	0.4658	0.3399	0.2676

Table 2. $(F_2)_{\text{new}}/(F_2)_{\text{old}}$

z_{0H}/z_{0M}	Ri_B			
	-0.25	-0.50	-0.75	-1.00
	0.9742	0.9437	0.9248	0.9113
	0.8396	0.7761	0.7396	0.7149
	0.6972	0.6057	0.5551	0.5215

Table 3. $(ch)_{\text{new}}/(ch)_{\text{old}}$

z_{0H}/z_{0M}	Ri_B			
	-0.25	-0.50	-0.75	-1
	0.4538	0.4396	0.4308	0.4245
	0.2854	0.2638	0.2514	0.2430
	0.1866	0.1621	0.1485	0.1396

When $|\mathbf{v}_2| = 0$, little change occurs in either cm and ch in a stable layer, except for the difference in numerical meaning of 'smallness.' Even under unstable stratification, cm is reduced only by a factor of 74/75, while ch is reduced by $1.06 \times (z_{0H}/z_{0M})$.

These changes have little effect on momentum transfer under all conditions, but reduce the transfer of both heat and water vapor between the atmosphere and the earth, especially under unstable stratification, from that obtained with the old specification.

2.2 Roughness Lengths Over Oceans

In UG-91, as well as in the current PL-GSM, the roughness length for momentum is calculated as

$$z_{0M} = \frac{a (1 + u_2^2 + v_2^2)}{\ln \frac{z_2}{b (1 + u_2^2 + v_2^2)}} \quad (14)$$

where $a = 3.0 \times 10^{-4}$, $b = 2.1 \times 10^{-6}$, both in the unit of sec^2/m , while (u_2, v_2) are the horizontal winds in m/s at the top of the surface layer, z_2 in meters. The roughness length for heat or water vapor is set equal to z_{0M} . Given the ocean surface temperature and assuming saturation of water vapor at the surface, the exchange coefficients in the surface layer are then evaluated according to the formulas given in Eqs. (1) - (7).

It is understood that Eq. (10) is an approximation to the solution of what we may call the Charnock equation for z_{0M} given by

$$z_{0M} = \frac{\alpha k^2}{g} \left(\frac{u}{\ln \frac{z}{z_{0M}}} \right)^2 \quad (15)$$

that arises from the logarithmic wind profile

$$u(z) = \frac{u_*}{k} \ln \frac{z}{z_{0M}} \quad (16)$$

subject to the constraint¹¹

$$gz_{0M} = \alpha u_*^2 \quad (17)$$

where g is the constant of gravity, u_* the friction velocity and $\alpha = 0.0184$.

We call Eq. (17) the Charnock formula and the parameter α the Charnock constant. Many different values for α have been suggested by different people, ranging from as small as 0.011 (Smith, 1980)¹² to as large as 0.072 (SethRaman and Raynor, 1975).¹³ The solutions of the Charnock equation for z_{0M} with different values of the Charnock constant are presented in Figure 1, where the abscissa V represents the wind speed $s = \sqrt{(1+V^2)}$ at 40 m above the surface. The curve E identified as PL-91 corresponds to that of Eq. (1). The corresponding friction velocities are shown in Figure 2. Closeness of C and E in both z_{0m} and u_* in these figures speaks well of the approximation represented by Eq. (1). We may also note that the difference in u_* between the two extreme values of the Charnock constant does not exceed 30 percent within the speed range of investigation.

The new formulas for roughness lengths are those recommended by Miller, Beljaars and Palmer [1992].⁹ They are given by

$$z_{0M} = \beta_1 \frac{v}{u_*} + \alpha_1 \frac{u_*^2}{g} = z_{sm} + z_{rm} \quad (18)$$

$$z_{0H} = \beta_2 \frac{v}{u_*} + \gamma_2 \quad (19)$$

$$z_{0Q} = \beta_3 \frac{v}{u_*} + \gamma_3 \quad (20)$$

where $\alpha = 0.018$, $\beta_1 = 0.11$, $\beta_2 = 0.40$, $\beta_3 = 0.62$, $\gamma = 1.4 \times 10^{-5}$, $\gamma = 1.3 \times 10^{-4}$, and v is the kinematic viscosity of the air, given the value of $1.5 \times 10^{-5} \text{ m}^2\text{s}^{-1}$. Friction velocity, u_* , satisfies the logarithmic wind profile equation,

$$u(z) = \frac{u_*}{k} \ln \frac{z}{z_{sm} + z_{rm}} \quad (21)$$

Substitution of Eq. (18) into Eq. (21) yields an equation that one may call the Charnock equation for u_* and reads

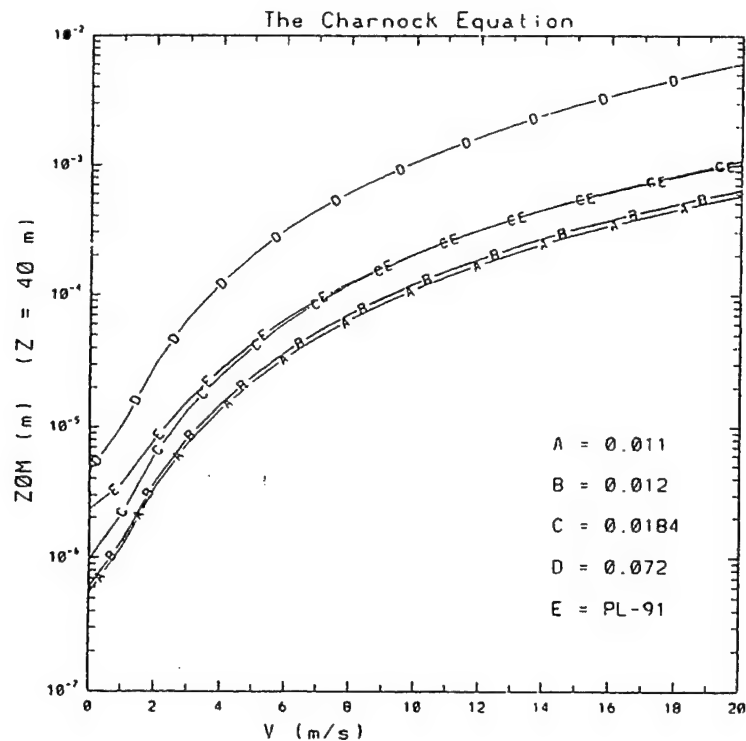


Figure 1. Roughness Length for Momentum, z_{0M} , as Solutions of the Charnock Equation for Different Values of the Charnock Constant, vs the Wind Speed V at 40 m Above Surface

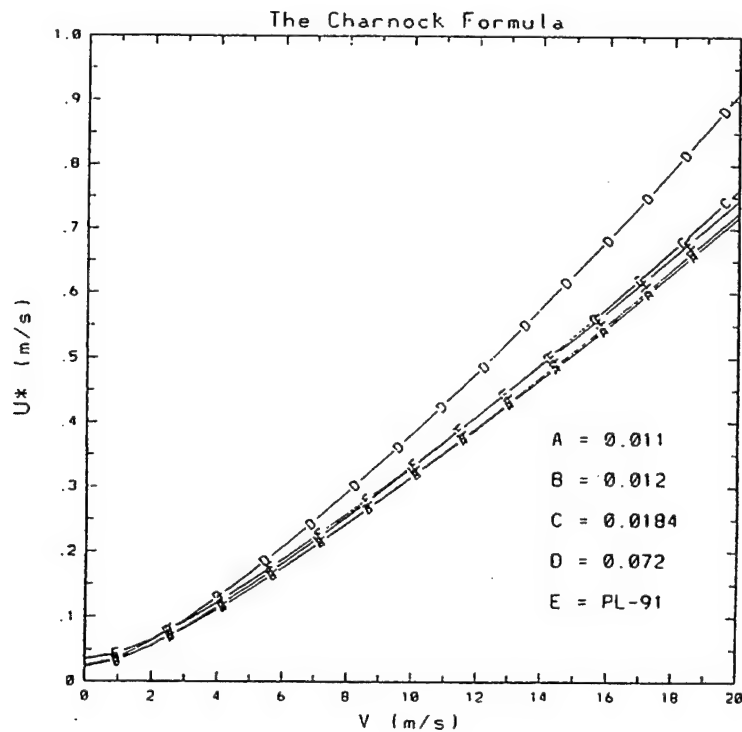


Figure 2. Friction Velocity, u_* , Corresponding to z_{0M} of Fig. 1, vs the Wind Velocity V at 40 m Above Surface

$$u_* \ln \frac{z}{\beta_1 \frac{v}{u_*} + \alpha_1 \frac{u_*^2}{g}} = k u(z) \quad (22)$$

The equation is solved for u_* with a given value of u at level z and the corresponding roughness lengths are then evaluated in accordance with Eqs. (18) - (20).

The three roughness lengths given by the new prescription are shown in Figures 3a and 3b. Comparisons of z_{OM} between the old and new formulas are presented in Figures 4a and 4b. It is readily seen in these figures that the new model prescribes different patterns of exchanges between near-calm and windy regimes over oceans, whereas the old version prescribes only monotonic changes. It is also apparent from Figure 5, which shows the ratios of these roughness lengths, that the new prescription over oceans is characteristically different from the counterpart over land where $z_{OH} = 0.01 \times z_{OM}$ has been suggested.

The most immediate and important effect of the changes in roughness lengths is seen in the surface layer exchange coefficients. We express the corresponding changes in these coefficients, under neutral stratification, by the ratio of the new to old values. We have, for momentum

$$\frac{cm(new)}{cm(old)} = \frac{N_1(new)}{N_1(old)} = \frac{\ln(z_2/z_{OM}(old))}{\ln(z_2/z_{OM}(new))}, \quad (23)$$

and for heat

$$\frac{ch(new)}{ch(old)} = \frac{N_2(new)}{N_2(old)} = \frac{R(old)}{R(new)} \cdot \frac{\ln(z_2/z_{OM}(old))}{\ln(z_2/z_{OM}(new))} \cdot \frac{\ln(z_2/z_{OH}(old))}{\ln(z_2/z_{OH}(new))} \quad (24)$$

where, it is recalled that $R(old) = 0.74$, $R(new) = 1.0$, and $z_{OH}(old) = z_{OM}(old)$. A similar expression holds for the ratio of cq . Figure 6 presents these ratios with $z_2 = 40$ m. It is apparent that all three exchanges in the surface layers are smaller in the new model than in the old except in the very low wind regime where exchanges of heat and water vapor are much more enhanced than that for momentum.

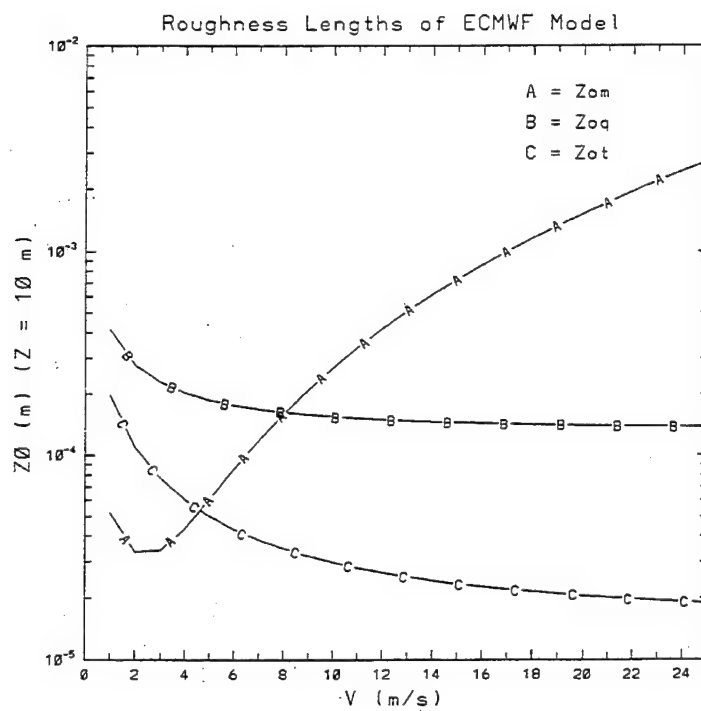
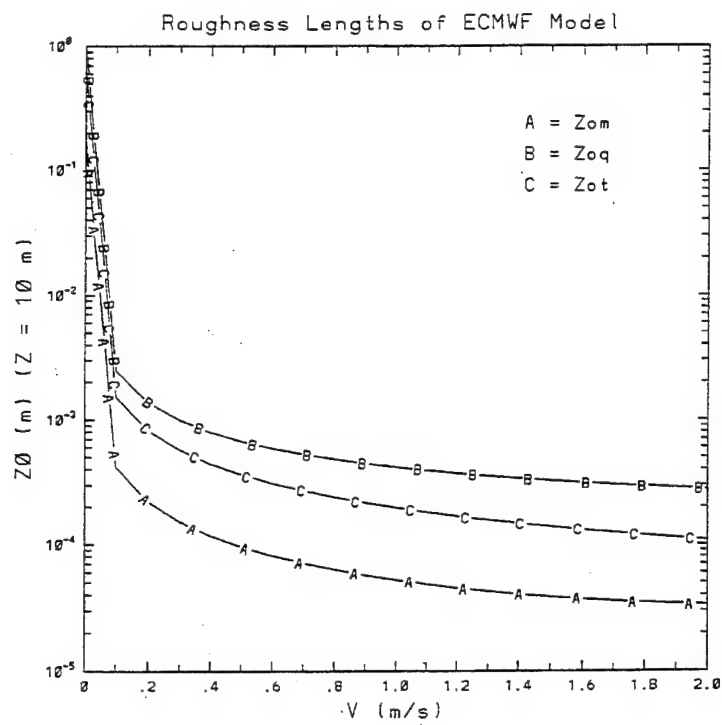


Figure 3. Roughness Lengths z_{0m} for Momentum, z_{0q} for Water Vapor, and z_{0t} for Heat vs Wind Speed V at 40 m Above Surface. (a) $2 \geq V > 0$, in m/s, (b) $25 \geq V \geq 1$, in m/s

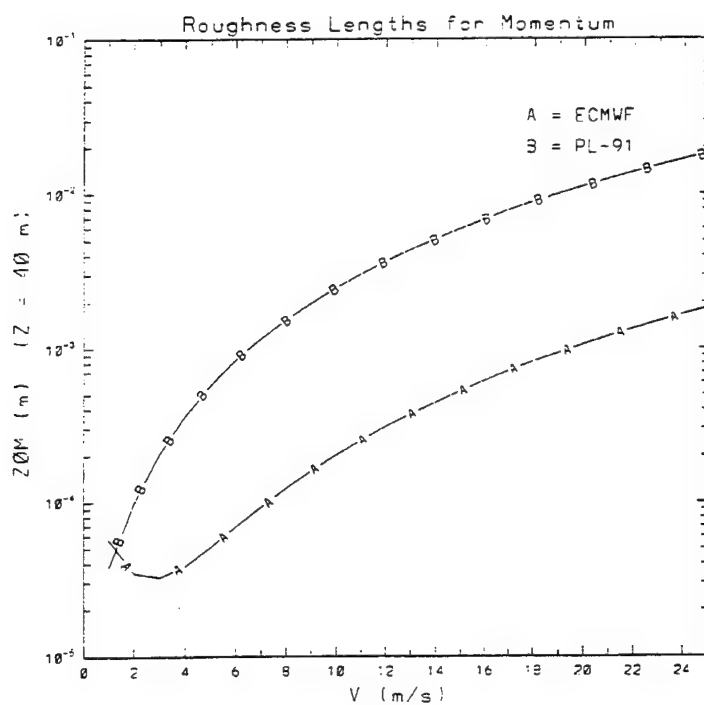
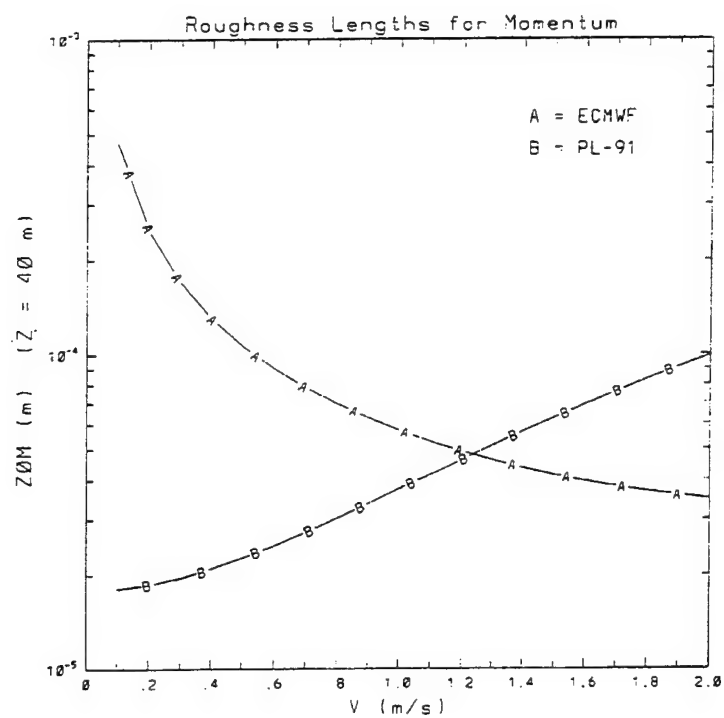


Figure 4. Roughness Lengths for Momentum, z_{0M} . A: ECMWF. B: PL-91.
(a) $2 \geq V > 0$, in m/s, (b) $25 \geq V \geq 1$, in m/s

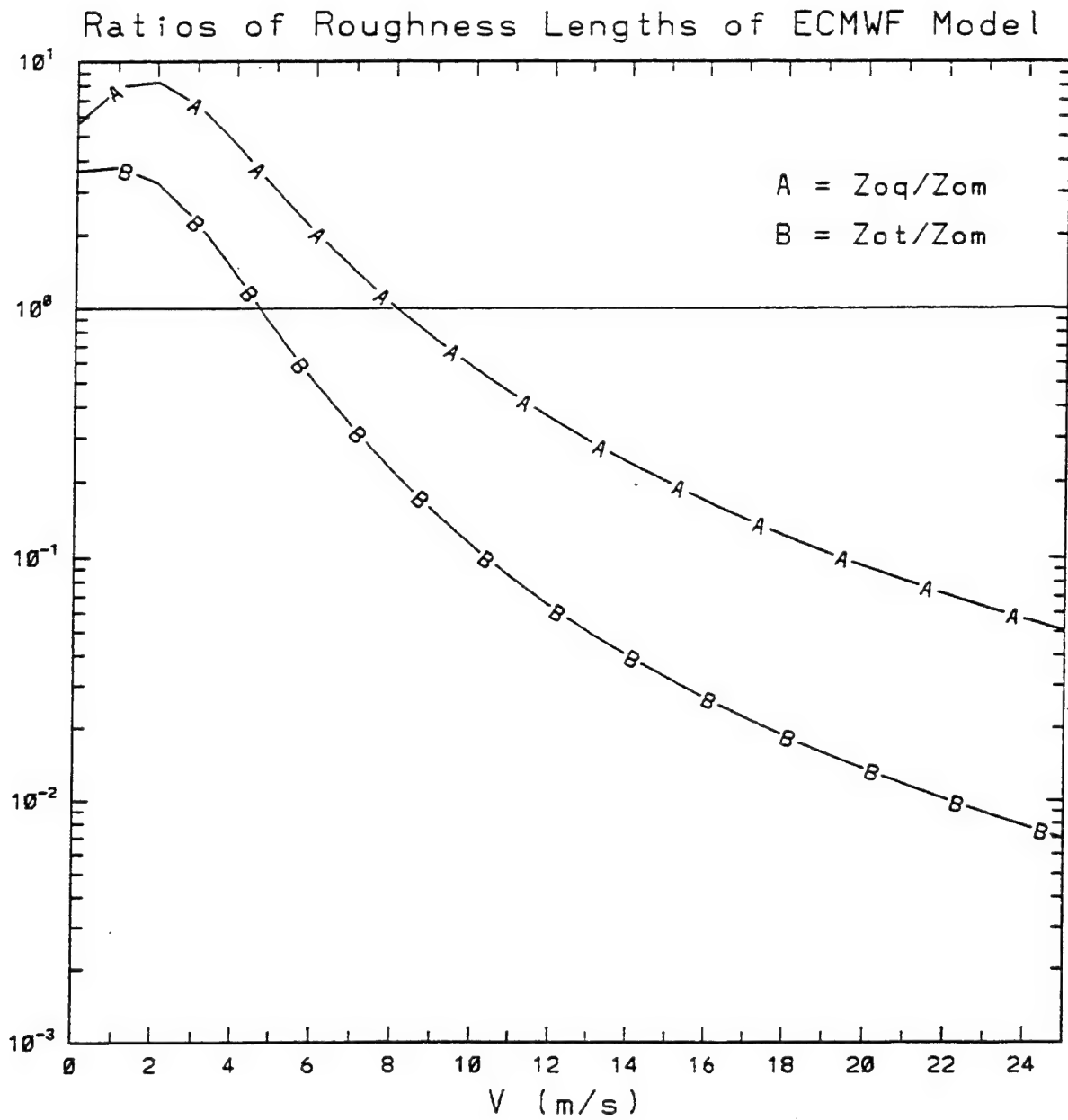


Figure 5. Ratio of Roughness Lengths, z_{oq}/z_{om} and z_{ot}/z_{om} According to the ECMWF Formulas

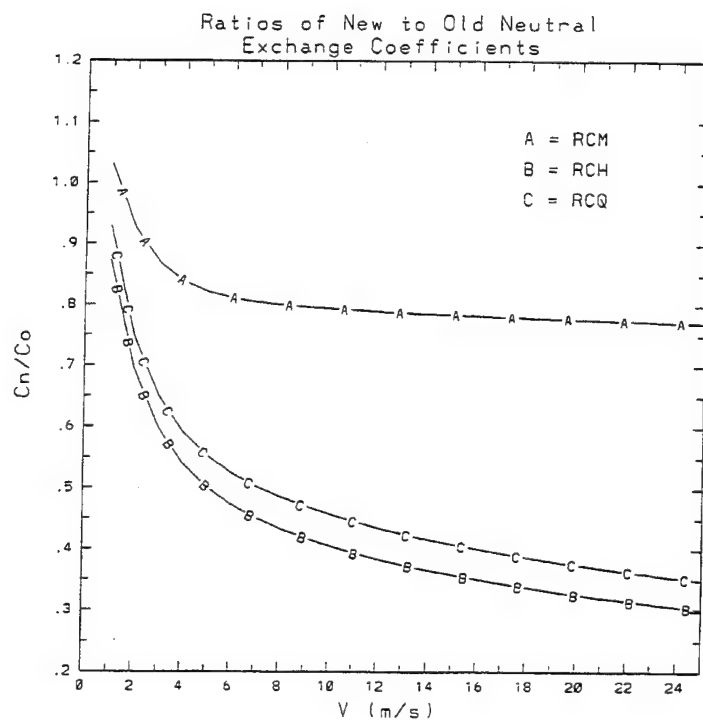
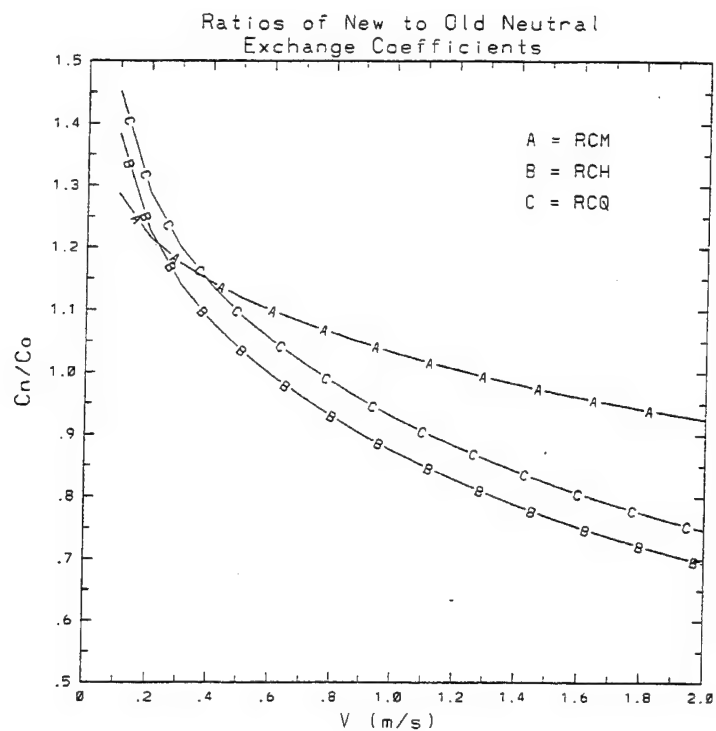


Figure 6. Ratios of the New to Old Exchange Coefficients: RCM for Momentum, RCH for Heat, and RCQ for Water Vapor. (a) $2 \geq V > 0$, in m/s, (b) $25 \geq V \geq 1$, in m/s

3. STRUCTURAL CHANGES

The driving force behind the structural changes arises from a new modeling of balance of energy fluxes at surface. The old version sets up the balance among four fluxes, namely, sensible heat, latent heat, upward radiative heat, and heat accompanied by precipitation for given downward radiative flux and soil heat flux, and solves for temperature and specific humidity at the surface. The solutions are next modified step by step as heat fluxes due to phase changes of precipitation and snow cover are taken into account. The new algorithm includes all energy transfers that are supposed to take place at the surface in the balance equation simultaneously and solves it for the temperature and specific humidity. As we restructure the balance equation we find it necessary at various junctures to introduce a new formulation or interpretation of terms representing quantities relevant to the energy balance. For both brevity and clarity it is thought best that we present the new model in its entirety first without reference to the old version and make comparative comments later as necessary.

3.1 Parametric Representation of Surface Energy Fluxes

(a) Downward radiative energy flux (FD) is given by

$$FD = (1 - \alpha) S + L \quad (25)$$

where α stands for albedo and S and L are short- and long-wave downward radiative fluxes, respectively. In the PL-GSM environment FD is calculated in the component of the model where all radiative transfers are modeled and evaluated prior to calling the boundary layer system.

(b) Sensible heat flux (H) is represented by

$$H = \rho c_p CH (T_s - \theta_2) \quad (26)$$

where ρ is air density in the surface layer (kg/m^3), c_p is the specific heat at constant

pressure of air ($\text{J/kg}^\circ\text{K}$), CH is the exchange coefficient for heat in the surface layer (m/s), T_s is the surface air temperature ($^\circ\text{K}$), and θ_2 is the potential temperature at the top of the surface layer ($^\circ\text{K}$).

(c) Soil heat flux (G) is defined by

$$G = k_0 \frac{T_s - Tb_1}{\frac{|zb_1|}{2} + esd \frac{\rho_w}{\rho_s} \frac{k_0}{k_s}}, \quad (27)$$

where k_0 and k_s are, respectively, the thermal conductivities of soil and of snow. Tb_1 is the temperature ($^\circ\text{K}$) at the midpoint of the first soil layer of thickness zb_1 (m) and esd snow depth expressed in equivalent water (m). ρ_w and ρ_s are densities of water and ice, respectively. The model thus represents the effect of snow cover as equivalent to that of an additional soil layer of depth proportional to k_0/k_s .

(d) Latent heat flux due to evaporation or sublimation (E) is given by

$$E = \rho L CQ(q_s - q_2), \quad (28)$$

where L is latent heat of evaporation (sublimation) if $T_s > T_{00}$ ($T_s \leq T_{00}$), in which T_{00} is the freezing point of water, taken to be 273.16 K. CQ is the exchange coefficient for water vapor in the surface layer (m/s) and q_s and q_2 are specific humidities (kg/kg) at surface and at the top of the surface layer, respectively.

(e) Upward radiative heat flux (FU) is given by

$$FU = \sigma (T_s)^4, \quad (29)$$

where σ is the Stefan-Boltzman constant.

(f) Heat flux brought by precipitation (Wp)

$$Wp = c_w (T_p - T_s) prcp, \quad (30)$$

where c_w is specific heat of water (J/kg K), T_p temperature of precipitation ($^\circ\text{K}$) and $prcp$ rate of precipitation ($\text{kg/m}^2 \text{ s}$).

(g) Flux of latent heat released or consumed as arriving precipitation undergoes a phase change is represented as follows:

(g1) when $T_s \leq T_{00}$

(g1a) if $T_p > T_{00}$, then the arriving rain is frozen with release of latent heat of fusion given by

$$Wc = L_f \text{ prcp}, \quad (31)$$

(g1b) if $T_p \leq T_{00}$ no phase change occurs and no realization of latent heat takes place.

In both cases, there results an accumulation of precipitation at the surface and the value of esd at the time step is changed to

$$\text{esd} = \text{esd} + \text{prcp} \, dt \times 10^{-3}. \quad (32)$$

(g2) when $T_s > T_{00}$

(g2a) if $T_p > T_{00}$ the arriving rain takes part in melting the existing snow cover, but there is no phase transformation and no release of latent heat by the precipitation.

(g2b) if $T_p \leq T_{00}$ the frozen precipitation melts by consuming latent heat of melting given by

$$Wc = - L_f \text{ prcp} \quad (33)$$

(h) Heat flux from melting of snow cover (Wm) is modeled as follows: when $T_s > T_{00}$, some of the existing snow cover melts at the expense of latent heat of melting, L_f . If it is assumed that the temperature of the entire snow cover is constant at T_s , then $\rho_w c_p (T_s - T_{00}) \text{ esd}$ is the amount of heat available per unit area for melting. The reduced snow depth in equivalent water dz is then given by $\rho_w L_f dz$. Equating the demand and supply, we then find

$$dz = c_s (T_s - T_{00}) \text{ esd} / L_f \quad (34)$$

With $c_s = 2.09 \times 10^3 \text{ J/(kg K)}$ and $L_f = 3.34 \times 10^5 \text{ J/kg}$, $dz/esd < 1$ as long as $T_s - T_{00} < 160^\circ \text{K}$. It is thus unlikely that any reasonable value of T_s would cause dz to be greater than esd . We assume, therefore, that when $T_s > T_{00}$, melting of snow cover requires an energy flux given by

$$Wm = \rho_w c_s (T_s - T_{00}) esd/dt \quad (35)$$

where dt is the size of a unit time step, in seconds.

The balance of energy fluxes at the surface can now be written as

$$FD + Wp + Wc = H + G + E + FU + Wm \quad (36)$$

where Wp and Wc are null when there is no precipitation and so is Wm when $T_s \leq T_{00}$.

While the surface energy given by Eq. (36) is balanced, the depth of snow cover may change, due possibly to the following two processes:

(1) sublimation, the energy flux of which is given by E , reduces the snow depth during the ensuing time step given by

$$dzs = \frac{1}{\rho_w} \frac{E dt}{L_f}, \quad (37)$$

(2) melting occurs only when $T_s > T_{00}$ and amounts over the time step to

$$dzm = \frac{c_s (T_s - T_{00}) esd}{L_f}. \quad (38)$$

3.2 Solving the Surface Energy Balance Equation

In solving Eq. (36) for surface temperature, T_s , and surface specific humidity, q_s , the following postulates and assumptions are made:

a. The profile conditions both in the atmosphere and in the soil at the time for which balance is sought are given.

b. The amount of the incoming radiative flux is known. Also known is the

condition of the surface as to whether it is covered with snow or not by the given value of *esd*.

- c. The type of precipitation is determined by (T_p, T_s) .
- d. The temperature of precipitation is set equal to the air temperature at the top of the surface layer, T_2 .
- e. Over land, the exchange coefficient for specific humidity in the surface layer has the same value as that for heat.
- f. Virtual temperature T_v is evaluated using

$$T_v = T (1 + 0.61 \times q), \quad (39)$$

where T is air temperature (°K) and q specific humidity.

- g. All snow covers are uniform and constant in all physical properties.
- h. Air density in the surface layer is evaluated according to

$$\rho = \frac{p_s + p_2}{R_a (T_{vs} + T_{v2})} \quad (40)$$

where p_s and p_2 are pressure at the surface and at the top of the surface layer, respectively, and T_{vs} and T_{v2} are the corresponding virtual temperatures. R_a denotes the gas constant for dry air.

- i. In the PL-GSM environment the lowest model-layer level identified by $p_2/p_s = 0.995$ is regarded as the top of the surface layer.

The solution procedure takes the following three steps:

- (1) solve the balance equation for potential evaporation, Ep , and the corresponding temperature, Tp ,
- (2) evaluate actual evaporation E as a fraction of Ep ,
- (3) solve the balance equation for surface temperature T_s , and surface specific humidity, q_s , corresponding to the actual evaporation E .

Even armed with the aforementioned premises regarding the conditions surrounding the surface, the surface energy balance equation as given in Eq. (36) is

obviously not linear in T_s and q_s , and one is presented with a number of alternative solution methods. We have in the present study experimented with two methods, one nonlinearly and the other by linearizing the balance equation, both of which employ iterations to satisfy prescribed threshold criteria. In the nonlinear solution, the Newton-Raphson algorithm is modified slightly to reduce the number of iterations required for meeting the criterion that the magnitude of imbalance be less than a specified value. The solution method for the linearized version is presented below to help tracing the codes of the subroutine executing the solution procedure.

Our first step is to solve Eq. (36) for potential evaporation Ep and the corresponding temperature Tp such that

$$T_s = Tp, \quad Ep = \rho L_v CQ (q^*(Tp, p_s) - q_2) \quad (41)$$

where $q^*(Tp, p_s)$ denotes the saturation specific humidity at temperature Tp and pressure p_s . This is accomplished by linearizing two energy fluxes FU and Ep at T_2 as follows:

$$FU = \sigma (T_2)^4 + 4\sigma (T_2)^3 (Tp - T_2), \quad (42)$$

$$Ep = \rho L_v CH \left(\frac{dq}{dT} \right) (Tp - T_2) + \rho L_v CQ (q^*(T_2, p_s) - q_2). \quad (43)$$

in which the approximation $q = \epsilon \cdot e/p$ is invoked, where e and p are vapor and air pressure, respectively, and ϵ the ratio of atomic weights water vapor and air. All other fluxes are linear in Tp , if one ignores the dependence of various coefficients such as ρ , CH and k_0 on Tp . The resulting system of equations for Ep and $(Tp - T_2)$ can be written as

$$Ep + A1 (Tp - T_2) = B1, \quad (44a)$$

$$Ep + A2 (Tp - T_2) = B2, \quad (44b)$$

where

$$A1 = \rho c_p CH + 4\sigma (T_2)^3 + \frac{k_0}{\frac{|zb_1|}{2} + esd} \frac{\rho_w k_0}{\rho_s k_w} + c_w prcp + d_1 \rho_s c_s \frac{esd}{dt} \quad (45)$$

$$A2 = -\rho L_v CH \left(\frac{dq}{dT} \right)_{T_2},$$

and

$$B1 = FD - \sigma (T_2)^4 - \rho c_p CH (T_2 - \theta_2) - \frac{k_0}{\frac{|zb_1|}{2} + esd} \frac{\rho_w k_0}{\rho_s k_s} (T_2 - Tb_1) + d_2 L_f prcp + d_1 \rho_s c_s \frac{esd}{dt} (T_2 - T_{00}) \quad (46)$$

$$B2 = -\rho L_v CH (q^*(T_2, p_s) - q_2)$$

in which

$$d_1 = \begin{pmatrix} 1 & \text{if } Tp > T_{00}, \\ 0 & \text{if } Tp \leq T_{00}, \end{pmatrix} \quad (47)$$

and

$$d_2 = \begin{pmatrix} 1 & \text{if } Tp_2 \leq T_{00}, \\ -1 & \text{if } Tp_2 > T_{00}. \end{pmatrix} \quad (48)$$

When there is snow cover at the surface, that is, $esd \neq 0$, evaporation is assumed to take place at the potential rate so that (Tp, Ep) defines the surface condition and individual energy fluxes are evaluated in accordance with the expressions given in the previous section.

When there is no snow cover at the surface, the actual rate of evaporation is evaluated next. In current practice, actual evaporation is made up of three components, namely, direct evaporation from bare soil, transpiration from vegetation, and evaporation from the canopy top. Each of these components is represented parametrically as a non-negative fraction of potential evaporation. With the total

actual rate of evaporation E given as the sum of the components, the surface energy balance equation, Eq. (44a,b) is recast as

$$E + A1 (T_s - T_2) = B1 \quad (49)$$

to yield the value of surface temperature T_s . The value of surface specific humidity q_s is then computed using

$$q_s = q_2 + \frac{E}{\rho \cdot CH} \quad (50)$$

The iteration starts with an arbitrary set of initial guesses and ends when magnitudes of individual energy fluxes as well as their imbalance between successive steps all become less than a prescribed tolerance limit.

3.3 Monteith's Psychrometer Constant

Monteith¹⁴ introduced an equation that reads

$$e_s(T_w) - e = \gamma (T - T_w) \quad (51)$$

which he credits to Brunt (1939)¹⁵ and calls γ the 'psychrometer constant'. Here, $e_s(T_w)$ is the saturation vapor pressure at temperature T_w and e and T are the water-vapor pressure and temperature of the air. We wish to determine the expression for γ and examine to what extent it can be regarded as a constant by starting from Brunt's original wet-bulb temperature equation. It is given by

$$(c_p + c_p'w)(T - T_w) = L_v(w' - w) \quad (52)$$

where c_p and c_p' are the specific heats at constant pressure of dry air and water vapor, respectively, w and T are the mixing ratio and temperature of the approaching air, while w' and T_w are those of the air leaving the wet-bulb thermometer. Treating both dry air and water vapor as perfect gases, we find

$$c_p' = \frac{8}{7\epsilon} c_p \quad (53)$$

where $\varepsilon = 0.622$ is the ratio of the molecular weight of water to that of air. Converting mixing ratios to water-vapor pressures using

$$w = \frac{\varepsilon e}{p - e}, \quad w' = \frac{\varepsilon e_s(T_w)}{p - e_s(T_w)}, \quad (54)$$

we obtain from Eq. (52) the following expression for γ :

$$\gamma = \frac{c_p p}{\varepsilon L_v} \frac{1 + \frac{1}{7} \frac{e}{p}}{1 + \frac{e_s(T_w)}{p - e_s(T_w)}} = \frac{c_p}{\varepsilon L_v} F \quad (55)$$

in which the second quotient, F , is seen to depend on p , e and $e_s(T_w)$ and may be readily shown to be always less than 1 but greater than $1 - [e_s(T_w)/p]$. The fractional excess error by regarding γ constant is, therefore, less than 5 percent of its true value even under extremely humid conditions typical of the tropics and much less in more common situations.

On the other hand, the mixing ratio in the atmosphere is often approximated by

$$w = \varepsilon \frac{e}{p} \quad (56)$$

If we use such an approximation in Eq. (52) we obtain

$$(c_p + \varepsilon \frac{e}{p} c_p')(T - T_w) = \frac{\varepsilon L_v}{p} [e_s(T_w) - e] \quad (57)$$

and the psychrometer constant γ becomes

$$\gamma = \frac{c_p p}{\varepsilon L_v} (1 + \frac{8}{7\varepsilon} w) \quad (58)$$

which shows the second quotient always greater than unity, in contradiction to what was found in Eq. (55). Thus, when the approximation Eq. (56) is adopted, the fractional deficit error of w is (e/p) and, according to Eq. (58), the fractional error in γ by regarding it constant is also negative and slightly greater in magnitude than w .

We think it better to use Eq. (58) for the expression of γ in the GSM environment.

3.4 Definition of Plant Coefficient

Mahrt et al.⁵ state that "the plant coefficient is formally defined here as the ratio of transpiration to the potential evaporation for the case of insignificant soil water deficit," and proceed to model transpiration, which is one of three components of actual evaporation, in terms of plant coefficient and other parameters at gridpoints over land. Plant coefficient in UG-91, on the other hand, is represented as a quantity that results from surface energy balance at a given time and a given location where evaporation incorporates the effect of plant resistance to evaporation.

We wish to define plant coefficient very much in the spirit of the first part of the Mahrt's phrase quoted above, but in a more explicit fashion that reflects intrinsic characteristics of the physiology of plants in question. We think such a definition is plausible when we interpret what Monteith¹⁴ regards as the evaporation from a dry leaf surface, $(L_v E)_{dry}$ as transpiration, while calling the evaporation from a wet surface, $(L_v E)_{wet}$ the potential evaporation as Penman¹⁶ did. According to Monteith, then, plant coefficient, pc , is defined by

$$pc = \frac{(E)_{dry}}{(E)_{wet}} = \frac{\Delta + \gamma}{\Delta + \gamma'} \quad (59)$$

where $\Delta = (de_g/dT)$, γ is the psychrometer constant defined in the previous paragraph, and $\gamma' = \gamma (1 + r_c \cdot cq)$, where r_c is a parameter in units of s/m representing the plant resistance to evaporation and cq the exchange coefficient for water vapor of the surrounding air.

3.5 Types of Precipitation at the Surface

The model employs two integer indices, `flgsn1` and `flgsn2`, to classify the type of precipitation as it arrives at the surface. A new method of classification which is

mutually exclusive and collectively exhaustive replaces those employed in UG-91 and PL-91. Denoting the temperature of precipitation by tp and temperatures of air at the top and bottom of the surface layer by $t2$ and $t1$, respectively, all expressed in $^{\circ}\text{C}$, the three different classifications are summarized in Table 4.

Table 4. The Old and New Classifications of Precipitation at the Surface.

tp : temperature ($^{\circ}\text{C}$) of the precipitation,
 $t1$: air temperature ($^{\circ}\text{C}$) at the surface,
 $t2$: air temperature ($^{\circ}\text{C}$) at the top of the surface layer.

	UG-91	PL-91	New
variables	$(tp, t1)$	$(tp, t2)$	$(tp, t1)$
rain	$tp > 0$ flgsn1 = 0 $t1 > 0$ flgsn2 = 0	$tp > 0$ flgsn1 = 0 $t2 > 0$ flgsn2 = 0	$tp > 0$ flgsn1 = 0 $t1 > 0$ flgsn2 = 0
freezing rain	$tp > 0$ flgsn1 = 0 $t1 \leq 0$ flgsn2 = 1	$tp > 0$ flgsn1 = 0 $t2 \leq 0$ flgsn2 = 1	$tp > 0$ flgsn1 = 0 $t1 \leq 0$ flgsn2 = 1
ice pellets		$tp \leq 0$ flgsn1 = 1 $t2 > 0$ flgsn2 = 1	$tp < 0$ flgsn1 = 0 $t1 > 0$ flgsn2 = 0
snow	$tp \leq 0$ flgsn1 = 1 $t1 \leq 0$ flgsn1 = 0	$tp \leq 0$ flgsn1 = 1 $t2 \leq 0$ flgsn2 = 1	$tp \leq 0$ flgsn1 = 1 $t1 \leq 0$ flgsn2 = 1

It is noted here that our current practice takes tp to be the same as $t2$, as UG-91 does, while PL-91 chose tp to be the air temperature at the model-layer level closest to 850 hPa. The choice of variables has been predicated on the assumption that falling precipitation attains thermodynamic equilibrium with everything else at the surface. It is, therefore, also implicit in the new classification that freezing rain accompanies release of heat of fusion, while ice pellets require consumption of heat of melting, either of which, whenever it occurs, is accounted for as W_c in the surface energy balance.

3.6 Boundary Conditions for the Evolution of Soil Temperature

The model prescribes the evolution of soil temperature by the classical heat conduction equation,

$$C \frac{\partial T_b}{\partial t} = \frac{\partial}{\partial z} \left\{ k_T \frac{\partial T_b}{\partial z} \right\} \quad (60)$$

where T_b is the soil temperature, t time, and z depth below surface, assigned negative. Heat capacity C , and thermal conductivity k_T , are regarded as functions of soil water content. The equation is solved using centered finite differencing in the vertical and the backward Crank-Nicholson scheme in time; in which, however, the values of parameters C and k_T are held the same between the two time steps during time integration.

Three modifications of the procedure given in UG-91 are introduced in the new model for physical reasons given below.

Firstly, as described in Section 3.2, the new model replaces snow cover by an equivalent thickness of soil whose thermal properties are those of the top soil layer. Thus, the depth of the bottom of the first soil layer becomes

$$z(1) = z_{soil}(1) - z(esd) \quad (61)$$

where

$$z(esd) = \frac{k_T(1)}{k_s} \frac{\rho_w}{\rho_s} esd \quad (62)$$

in which k_s is the thermal conductivity of snow, and ρ_w and ρ_s are the densities of water and snow, respectively.

Secondly, in the PL-GSM land surface specification scheme, the soil temperature at $z = -2$ m is regarded as a constant with time that varies geographically according to annual climatology. The soil temperature in the second layer ($-1.00\text{m} < z < -0.05\text{m}$) is, therefore, affected not only by the heat flux at the upper boundary but also by that at the lower boundary surface which varies in time due to the change of the temperature

in the layer.

Finally, an analysis of the codes in UG-91 reveals that in setting the boundary condition at the surface required for stepping forward in time, an assumption regarding temperature changes at the surface is made of the form,

$$T_s^{n+1} - T_s^n = \frac{zz^n}{1 + zz^n} (T_{b1}^{n+1} - T_{b1}^n) \quad (63)$$

in which T_s and T_{b1} are the temperatures at the surface and in the first soil layer, respectively, the superscript denotes the time step referred to, and

$$zz^n = \frac{k_T}{\rho c_p ch + 4 \sigma T_2^3} \quad (64)$$

Since $zz^n > 0$ for all n , Eq. (63) implies that the temperature change at the surface is smaller than the corresponding change in the first soil layer at all times. We do not consider this realistic. In its place, we propose a tentative assumption for time integration of soil temperature that holds

$$G^{n+1} = G^n \quad (65)$$

that is, the ground-heat flux at the surface remains the same as the flux that results from surface energy balance at the start of the time interval. It is used only to update the soil temperature, whose change is generally much smaller than that of the surface temperature, to the next time step where the surface temperature and the corresponding ground-heat flux are calculated afresh as solutions of the surface energy balance under the new set of profile conditions.

4. EXPERIMENTS

We have chosen a region (shown in Figure 7) in the southern United States east of the Rockies between 28° and 38° N for a preliminary study in which we attempt to gauge the immediate impacts of formal and structural changes described in the

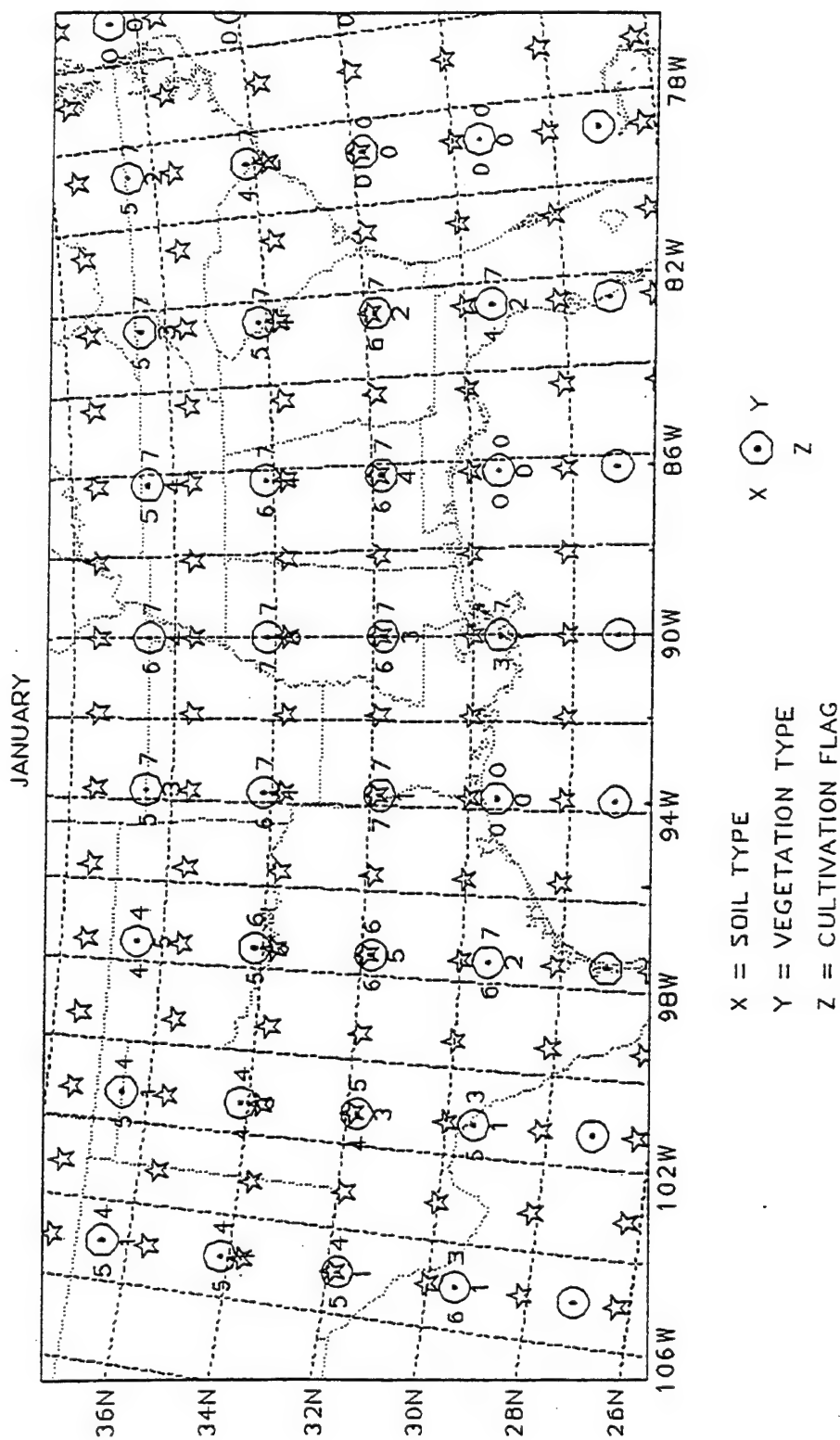


Figure 7. A Map of Model Gridpoints in the Region of Study, Southeastern United States. Each Gridpoint is Associated With Three Indices of Land Specification

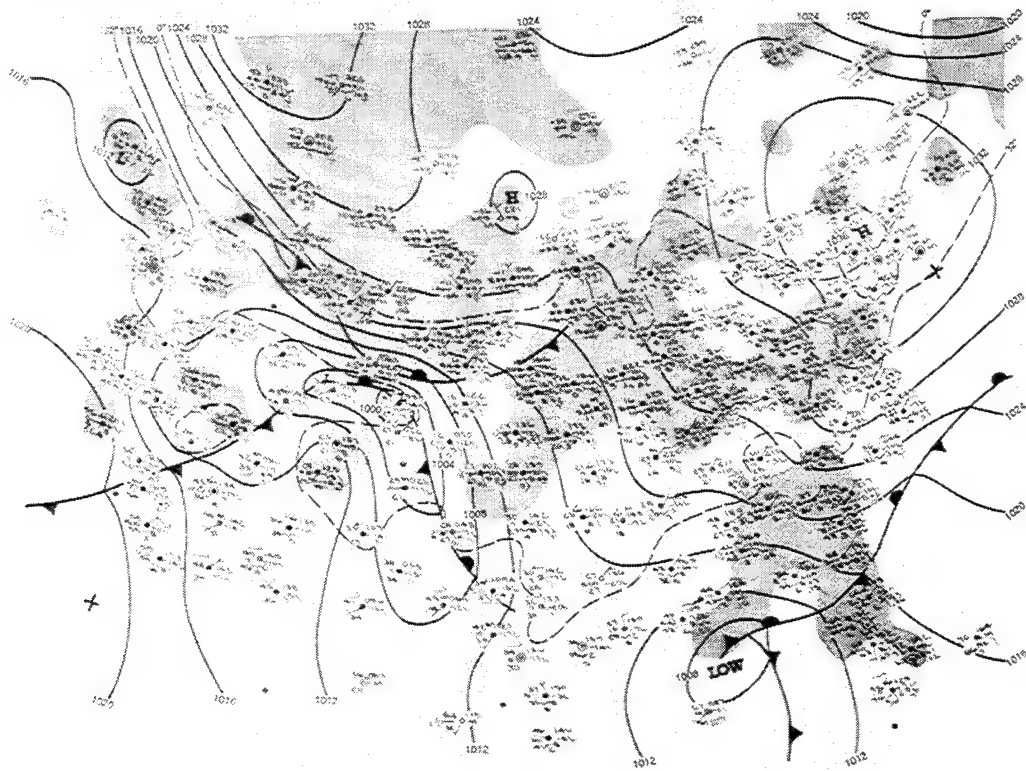
preceding sections on model outputs at the surface over land. In an earlier study with PL-GSM that used the FGGE-IIIb data we saved all outputs at each of the model gridpoints (marked by \odot in Figure 7) in the region that are considered relevant to the boundary layer system on every time step (20 min.) in the period between Jan 12 12 UTC and Jan 15 12 UTC of 1979. These outputs provide the profile conditions and other synoptic information at a given time required for evaluating surface variables and their influences on subsequent changes in the profile conditions. Also shown in Figure 7 are the three integer indices to each model gridpoint, representing the types of soil, vegetation, and cultivation of the area represented by the gridpoint. For presentation of the results of the experiments, we have named the model gridpoints by a pair of integer indices (i, j), in which i designates the west-to-east coordinate, starting with 1 at 105 W and ending with 9 at 75 W, and j represents the north-to-south coordinate, beginning with 1 slightly north of 36 N and ending with 4 just north of 29 N (see Figure 7).

A series of daily 7 a.m. EST (12 UTC) surface weather maps published by NOAA, shown in Figure 8, illustrates the weather over the United States during the period of study. It shows that a passing of two successive low-pressure centers and fronts brought much clouds and precipitation over most of the region. The simulation by the PL-GSM produced precipitation at all gridpoints east of 98°W every day in the form of heavy rainfall from late on the 12th to the afternoon of the 14th in the area east of 90°W. The radiation scheme in the model produced daily maximum downward radiative fluxes ranging from 600 to 910 w/m² in the region during this period.

In the present study we limited our scope to static tests where we were interested only in the outputs at the surface as the result of surface energy balance rather than in the dynamic impacts on the evolution of the entire GSM. We also limited our comparisons only to land gridpoints, since only 8 of the 36 gridpoints in the region are over oceans.

We have looked into two changes in form; surface-layer exchange coefficient and plant coefficient, and two changes in structure; composition in surface energy balance and solution algorithm for surface energy balance. A typical test was carried out on

FRIDAY, JANUARY 12, 1979



SATURDAY, JANUARY 13, 1979

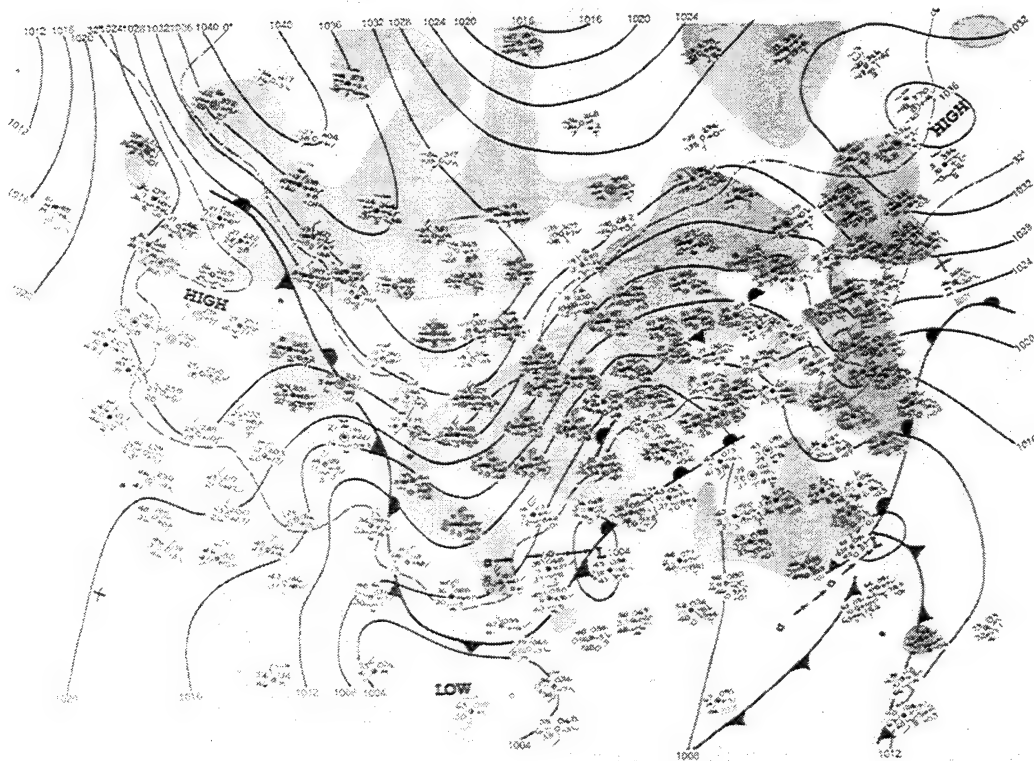


Figure 8. A Series of Weather Maps Over the United States During the Period of Study, Jan. 12, 12 UTC - Jan. 15, 12 UTC, 1979

SUNDAY, JANUARY 14, 1979



MONDAY, JANUARY 15, 1979

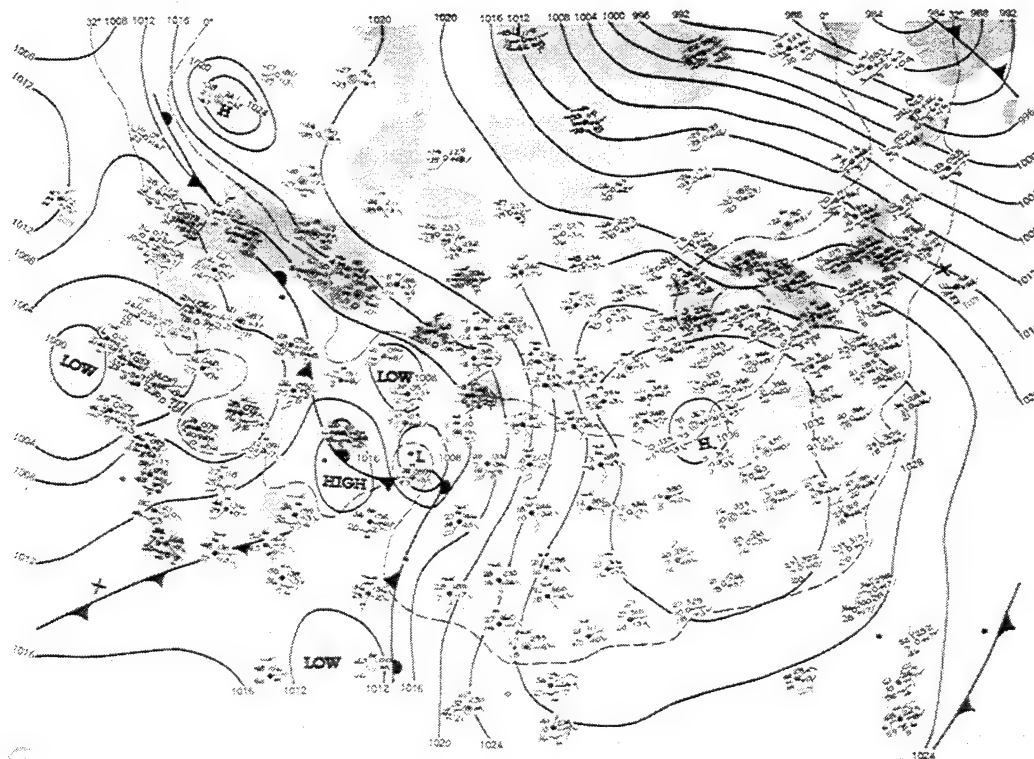


Figure 8 (Cont). A Series of Weather Maps Over the United States During the Period of Study, Jan. 12, 12 UTC - Jan. 15, 12 UTC, 1979

a 2×2 matrix of compatible models with two different attributes in which each attribute has the old and new versions. Employing parallel pairs allows us to gauge the sensitivity of the impacts to changes in the background.

We have found temperature, humidity and fluxes of sensible heat, ground heat and latent heat of evaporation to be the most telling among all the surface variables of differences between any pair of comparable models. We employ, therefore, differences in these variables to describe impacts of the changes imposed.

4.1 Plant Coefficient

Impacts from the change in evaluating plant coefficients were examined using the old structure. Tables 5 and 6 present examples of the contrasts in output at two different times of day, early morning and early afternoon, between the old and new plant coefficients when the model uses the old exchange-coefficient formulas. Tables 7 and 8 do the same for the model with the new exchange coefficients.

We note, first of all, that regardless of time and location and irrespective of exchange coefficients, the new value is larger than the old. The excesses in fraction of a few percentage points with the old exchange coefficients are smaller than those of mostly several percentage points with the new. We see, however, hardly any difference in either temperature or specific humidity due to the increased values of plant coefficient with either exchange coefficient. Differences found in these examples are no more than a hundredth of 1°K in temperature and a hundredth of 1 g/kg in humidity.

The impacts are more noticeable in the surface fluxes, but their magnitudes are still of no significance. The largest difference among all the three fluxes in the tables is 2.20 w/m^2 which is 1.5 percent of the flux value, and most of the flux differences are much smaller fractions of the corresponding flux values.

Table 5. A Comparison of Surface Outputs Between the Old (UG-91) and New Plant-coefficient Formulations With the Old Exchange Coefficients at Timestep = 1.

	(1,1)	(2,1)	(3,1)	gridpoints				
	(1,1)	(2,1)	(3,1)	(4,1)	(5,1)	(6,1)	(7,1)	(8,1)
1. Plant coefficient								
old	0.0363	0.1796	0.0610	0.0388	0.0706	0.0735	0.0531	0.0556
new	0.0370	0.1915	0.0619	0.0390	0.0716	0.0747	0.0536	0.0561
2. Surface temperature (T - 200 in K)								
old	74.94	74.73	74.14	72.31	73.09	74.22	73.08	74.14
new	74.94	74.73	74.14	72.31	73.09	74.22	73.08	74.14
3. Surface specific humidity (g/kg)								
old	4.55	4.60	4.12	3.02	3.56	3.86	3.51	3.76
new	4.55	4.60	4.12	3.02	3.56	3.86	3.51	3.76
4. Sensible heat flux (w/m*m)								
old	-204.35	-97.62	-40.68	368.93	129.34	60.14	161.34	200.01
new	-204.39	-97.63	-40.68a	368.92	129.31	60.10	161.30	199.97
5. Ground heat flux (w/m*m)								
old	19.78	1.61	-48.60	-429.70	-350.91	-314.88	-393.50	-348.19
new	19.75	1.60	-48.60	-429.70	-350.94	-314.94	-393.53	-348.22
6. Latent heat flux of evaporation (w/m*m)								
old	105.39	18.01	55.73	35.86	173.73	201.57	249.18	160.27
new	105.47	18.03	55.74	35.86	173.80	201.66	249.26	160.34
	(1,3)	(2,3)	(3,3)	gridpoints				
	(1,3)	(2,3)	(3,3)	(4,3)	(5,3)	(6,3)	(7,3)	(8,3)
1. Plant coefficient								
old	0.0530	0.1018	0.0751	0.0621	0.0485	0.0451	0.0442	
new	0.0545	.1060	0.0764	0.0628	0.0489	0.0454	0.0444	
2. Surface temperature (T - 200 in K)								
old	82.03	80.86	78.12	76.64	79.09	82.57	84.84	
new	82.03	80.85	78.12	76.64	79.09	82.57	84.84	
3. Surface specific humidity (g/kg)								
old	4.66	6.33	5.41	4.14	5.32	7.34	8.56	
new	4.66	6.33	5.41	4.14	5.32	7.34	8.56	
4. Sensible heat flux (w/m*m)								
old	-166.43	-171.85	25.19	314.96	145.79	79.35	241.11	
new	-166.46	-171.88	25.18	314.88	145.75	79.35	241.11	
5. Ground heat flux (w/m*m)								
old	30.12	-6.52	-162.30	-573.18	-436.35	-140.22	-14.65	
new	30.12	-6.53	-162.30	-573.25	-436.38	-140.22	-14.65	
6. Latent heat flux of evaporation (w/m*m)								
old	30.02	78.13	95.13	223.64	313.69	66.48	-224.09	
new	30.06	78.17	95.15	223.79	313.76	66.49	-224.09	

Table 6. A Comparison of Surface Outputs Between the Old (UG-91) and New Plant-coefficient Formulations With the Old Exchange Coefficients at Timestep = 19.

	(1,1)	(2,1)	(3,1)	gridpoints				
				(4,1)	(5,1)	(6,1)	(7,1)	(8,1)
1. Plant coefficient								
old	0.0413	0.0668	0.0635	0.0679	0.0774	0.0806	0.0860	0.0754
new	0.0421	0.0683	0.0645	0.0689	0.0788	0.0821	0.0877	0.0766
2. Surface temperature (T - 200 in K)								
old	77.83	79.88	78.21	77.28	79.97	81.01	78.79	79.22
new	77.83	79.88	78.21	77.28	79.97	81.01	78.79	79.22
3. Surface specific humidity (g/kg)								
old	5.48	5.66	4.92	4.50	5.57	6.14	5.61	5.77
new	5.48	5.66	4.92	4.50	5.57	6.14	5.62	5.77
4. Sensible heat flux (w/m*m)								
old	174.47	112.59	132.76	183.01	152.79	145.30	128.37	113.83
new	174.41	112.56	132.75	182.96	152.74	145.26	128.35	113.82
5. Ground heat flux (w/m*m)								
old	74.42	37.20	-18.95	-2.11	16.07	26.27	-12.61	-10.80
new	74.38	37.19	-18.96	-2.15	16.03	26.24	-12.63	-10.81
6. Latent heat flux of evaporation (w/m*m)								
old	112.54	201.41	243.60	181.08	188.11	180.16	140.71	151.13
new	112.54	201.44	243.63	181.17	188.20	180.24	140.76	151.16
	(1,3)	(2,3)	(3,3)	gridpoints				
				(4,3)	(5,3)	(6,3)	(7,3)	(8,3)
1. Plant coefficient								
old	0.0549	0.0707	0.0746	0.0899	0.0703	0.0596	0.0682	
new	0.0565	0.0726	0.0759	0.0915	0.0712	0.0604	0.0697	
2. Surface temperature (T - 200 in K)								
old	86.04	85.98	83.61	83.16	85.30	86.61	87.29	
new	86.04	85.98	83.61	83.16	85.30	86.61	87.29	
3. Surface specific humidity (g/kg)								
old	4.59	6.17	6.88	6.42	7.92	9.58	10.07	
new	4.59	6.17	6.88	6.42	7.92	9.58	10.07	
4. Sensible heat flux (w/m*m)								
old	264.36	158.60	187.05	265.34	280.76	200.70	102.70	
new	264.31	158.55	187.02	265.24	280.70	200.70	102.70	
5. Ground heat flux (w/m*m)								
old	60.81	43.75	-15.13	27.69	32.68	32.50	2.32	
new	60.80	43.73	-15.15	27.60	32.64	32.50	2.32	
6. Latent heat flux of evaporation (w/m*m)								
old	30.77	153.67	299.63	180.86	222.59	293.38	154.34	
new	30.83	153.74	299.69	181.04	222.70	293.38	154.34	

Table 7. A Comparison of Surface Outputs Between the Old (UG-91) and New Plant-coefficient Formulations With the New Exchange Coefficients at Timestep = 1.

	(1,1)	(2,1)	(3,1)	gridpoints				
				(4,1)	(5,1)	(6,1)	(7,1)	(8,1)
1. Plant coefficient								
old	0.0894	0.3446	0.1486	0.1421	0.2980	0.2431	0.1725	0.1846
new	0.0941	0.3864	0.1542	0.1461	0.3169	0.2570	0.1792	0.1917
2. Surface temperature (T - 200 in K)								
old	74.52	73.93	74.25	74.21	74.27	75.05	74.30	75.30
new	74.52	73.93	74.25	74.21	74.27	75.05	74.30	75.30
3. Surface specific humidity (g/kg)								
old	4.44	3.86	4.12	3.05	5.72	5.25	4.71	4.72
new	4.44	3.86	4.12	3.05	5.74	5.26	4.71	4.73
4. Sensible heat flux (w/m*m)								
old	-92.19	-44.82	-10.64	168.10	39.81	31.74	82.83	89.00
new	-92.24	-44.89	-10.65	168.10	39.72	31.65	82.71	88.86
5. Ground heat flux (w/m*m)								
old	-12.45	-17.24	-43.60	-213.54	-204.76	-209.50	-235.50	-202.99
new	-12.54	-17.24	-43.60	-213.56	-205.36	-209.97	-235.91	-203.43
6. Latent heat flux of evaporation (w/m*m)								
old	27.50	-12.06	20.21	12.05	111.74	120.75	164.15	120.80
new	27.64	-12.06	20.22	12.08	12.46	21.34	164.69	121.39
	(1,3)	(2,3)	(3,3)	gridpoints				
				(4,3)	(5,3)	(6,3)	(7,3)	(8,3)
1. Plant coefficient								
old	0.1217	0.2186	0.1981	0.2203	0.1398	0.1231	0.1220	
new	0.1303	0.2393	0.2087	0.2302	0.1444	0.1267	0.1250	
2. Surface temperature (T - 200 in K)								
old	80.22	80.20	78.78	78.50	80.08	82.85	84.87	
new	80.22	80.20	78.77	78.49	80.07	82.85	84.87	
3. Surface specific humidity (g/kg)								
old	4.87	5.88	5.83	6.01	6.34	7.64	8.61	
new	4.87	5.88	5.83	6.03	6.34	7.64	8.61	
4. Sensible heat flux (w/m*m)								
old	-126.52	-78.67	27.20	124.89	95.59	43.69	80.45	
new	-126.55	-78.67	27.16	124.57	95.43	43.65	80.45	
5. Ground heat flux (w/m*m)								
old	0.10	-23.90	-133.28	-354.45	-304.47	-109.20	-13.32	
new	0.08	-23.91	-133.33	-355.57	-304.82	-109.25	-13.32	
6. Latent heat flux of evaporation (w/m*m)								
old	29.47	5.71	60.97	186.33	227.23	69.73	-64.90	
new	29.53	5.73	61.06	187.83	227.76	69.82	-64.90	

Table 8. A Comparison of Surface Outputs Between the Old (UG-91) and New Plant-coefficient Formulations With the New Exchange Coefficients at Timestep = 19.

	(1,1)	(2,1)	(3,1)	gridpoints (4,1)	(5,1)	(6,1)	(7,1)	(8,1)
1. Plant coefficient								
old	0.1124	0.2242	0.1931	0.2101	0.2587	0.2702	0.3072	0.2197
new	0.1197	0.2429	0.2033	0.2204	0.2759	0.2897	0.3311	0.2315
2. Surface temperature (T - 200 in K)								
old	79.39	83.66	80.74	78.98	81.74	82.79	80.35	80.29
new	79.39	83.65	80.74	78.98	81.73	82.79	80.35	80.29
3. Surface specific humidity (g/kg)								
old	6.06	6.87	5.89	5.57	7.16	7.79	7.39	6.73
new	6.07	6.87	5.89	5.58	7.17	7.80	7.40	6.73
4. Sensible heat flux (w/m*m)								
old	100.96	101.24	111.31	96.88	72.99	69.11	51.14	63.48
new	100.79	101.15	111.25	96.73	72.83	68.96	51.06	63.41
5. Ground heat flux (w/m*m)								
old	175.11	125.38	96.48	132.78	146.88	148.40	96.25	71.70
new	174.72	125.29	96.38	132.36	146.34	147.91	95.89	71.52
6. Latent heat flux of evaporation (w/m*m)								
old	77.87	106.16	137.50	124.27	128.50	125.43	101.46	113.62
new	78.47	106.36	137.67	124.86	129.25	126.09	101.92	113.87
	(1,3)	(2,3)	(3,3)	gridpoints (4,3)	(5,3)	(6,3)	(7,3)	(8,3)
1. Plant coefficient								
old	0.1742	0.2676	0.2863	0.3460	0.2164	0.1647	0.1769	
new	0.1921	0.2988	0.3100	0.3733	0.2282	0.1737	0.1902	
2. Surface temperature (T - 200 in K)								
old	90.67	89.72	87.92	85.71	87.32	87.66	87.85	
new	90.66	89.71	87.91	85.68	87.31	87.66	87.85	
3. Surface specific humidity (g/kg)								
old	5.05	8.20	9.30	9.06	9.57	11.12	10.85	
new	5.06	8.21	9.31	9.11	9.58	11.12	10.85	
4. Sensible heat flux (w/m*m)								
old	163.95	88.04	117.68	88.54	141.02	112.07	60.46	
new	163.79	87.89	117.51	88.17	140.70	112.07	60.46	
5. Ground heat flux (w/m*m)								
old	136.68	140.73	160.73	229.59	188.77	132.95	48.84	
new	136.55	140.48	160.38	227.86	188.03	132.95	48.84	
6. Latent heat flux of evaporation (w/m*m)								
old	31.73	107.95	171.42	142.98	195.90	274.61	144.88	
new	32.05	108.40	171.97	145.18	197.02	274.61	144.88	

These results led us to conclude that the difference in the definition of plant coefficient would not produce any significant changes in values of surface variables to affect the rest of the model.

4.2 Exchange-Coefficient Formulas and Energy-Balance Algorithm

Impacts of the change in the formulas for surface-layer exchange coefficients and of the change in the procedure seeking the balance of surface energy fluxes are examined with the use of a 2-by-2 matrix of the following four models schematically depicted in Table 9.

Table 9. Schematic Diagram of Impact Evaluation.

		(formulas)	
		old	new
(algorithm)	old	A1	A2
	new	B1	B2

As we started looking into details of surface outputs from these models, we soon became alarmed by occasional appearances of incredibly large magnitudes of ground heat flux in models A1 and A2, but not in models B1 and B2. The anatomy of intermediate and final outputs revealed that such occurrences were invariably accompanied by the concurrence of two external conditions: the temperature at the lowest model-layer level, T_2 , is lower than the freezing point of water, T_{00} , and the rate of precipitation, $prcp$, is nonzero. It is recalled that our model assumes the temperature of precipitation as it arrives at the surface to be equal to T_2 . This fact and also the corresponding values of other surface parameters such as surface temperature and evaporative latent-heat flux led us to identify a particular segment in the old algorithm as the direct culprit of the phenomenon. The segment recalculates surface temperature and ground heat flux when it is judged that the surface is covered with

snow. We thus came to conclude that the old algorithm cannot adequately take account of surface conditions in accordance with the model premises when the conditions described above, namely, $T_2 < T_{00}$ and $\text{prcp} > 0$, occurs. Consequently, further comparisons among the models exclude all the gridpoints in the region that produced at any time step during the three days of the study an obviously incredible value of ground heat flux and a large value of imbalance.

We perceived either change depicted in Table 9 to be a minor modification to the entire framework of specifying the surface layer and, therefore, thought that we might regard each change as a perturbation and subject its impact on the surface parameters to a linear analysis. The pairwise comparisons afforded by the matrix can determine the extent to which such supposition may be valid. Such an approach might then enable us to discover certain general characteristics in the impact that are independent of differences in the other attribute and/or other influences such as synoptic or soil conditions.

Tables 10-13 present three statistics: mean, standard deviation of, and correlation between the models, on the daily basis (12 UTC-12 UTC) in four surface variables, namely temperature ($^{\circ}\text{C}$), specific humidity (g/kg), sensible heat flux and evaporative latent heat flux ($\text{w/m}^2\cdot\text{m}$), at four gridpoints: (2,2) (2,4), (7,2) and (7,4). The four gridpoints together cover well not only the spreads of geographical and weather conditions but also those of soil and vegetation of the region (see Figure 7). Part a in each of the tables gives the statistics of the variables themselves while part b those of differences between models of the individual variables.

We find, first of all, from part a that the daily statistics generally exhibit good parallelism between models across the changes. In temperature, t_1 , and sensible heat flux, H , correlations are uniformly very high between any pair among all four models at all gridpoints; supporting the notion that effects of the changes can be regarded as perturbations. In specific humidity, q_1 , and evaporative latent heat flux, E , however, the pair of gridpoints in the west: (2,2) and (2,4) presents significantly lower correlation than those in the east where the relations are as good as those found in temperature and sensible heat flux.

Table 10a. Summary Tables of Statistics of Models A1, A2, B1, and B2 at Gridpoint (2,2) for Variables t1 and q1

Summary Tables of Statistics of Models A1, A2, B1 and B2 at (2,2)									
1. Means (m) and standard Deviations (s)									
	t1			q1			H		
	A1	A2	B1	B2	A1	A2	B1	B2	E
day1	m	9.35	9.54	10.31	10.19	5.98	6.14	5.34	5.42
	s	4.53	5.05	4.81	5.52	0.65	1.08	0.46	0.52
day2	m	3.11	3.53	4.28	4.69	3.62	4.01	2.93	2.96
	s	3.46	4.27	3.90	5.00	0.52	0.78	0.60	0.58
day3	m	1.69	1.92	3.00	2.99	3.37	3.55	2.63	2.65
	s	2.92	3.22	3.33	3.75	0.17	0.46	0.22	0.21
2. Correlation Coefficients (r)									
	A1			A2			B1		
	day1	day2	day3	day1	day2	day3	day1	day2	day3
A1									
A2	.60								
B1	.85	.26							
B2	.86	.07	.03						
The values in the upper (lower) triangle are for t1- (q1-) correlations.									
2. Correlation Coefficients (r)									
	A1			A2			B1		
	day1	day2	day3	day1	day2	day3	day1	day2	day3
A1									
A2	.98								
B1	.99	.98							
B2	.99	.98	.98						
The values in the upper (lower) triangle are for H- (E-) correlations.									
Summary Tables of Statistics of Models A1, A2, B1 and B2 at (2,2)									
1. Means (m) and standard Deviations (s)									
	m			s			H		
	A1	A2	B1	A1	A2	B1	A1	A2	B1
day1	m	-63.5	-20.2	-12.2	-4.6	96.5	46.8	11.8	9.1
	s	90.4	49.5	107.9	58.2	66.2	58.5	25.8	19.0
day2	m	-40.6	-4.2	48.0	30.9	123.9	73.3	2.3	2.7
	s	119.7	63.6	146.5	87.2	76.2	71.0	1.3	2.1
day3	m	-104.9	-31.0	2.0	3.1	155.6	73.9	3.8	3.0
	s	87.0	46.8	88.7	57.0	64.5	47.6	3.8	2.0
2. Correlation Coefficients (r)									
	A1			A2			B1		
	day1	day2	day3	day1	day2	day3	day1	day2	day3
A1									
A2	.90								
B1	.86	.96							
B2	.80	.94	.99						
The values in the upper (lower) triangle are for H- (E-) correlations.									

Table 10b. Same as in Table 10a, Except for Variables H and E

Summary Tables of Statistics of Models A1, A2, B1 and B2 at (2,2)												
1. Means (m) and standard Deviations (s)												
	t1				q1				H			
	D1	D2	D3	D4	D1	D2	D3	D4	D1	D2	D3	D4
day1	m	.19	-.12	.96	.65	.15	.08	-.64	-.72			
	s	1.03	1.21	.55	.66	.87	.16	.35	1.01			
day2	m	.42	.41	1.17	1.16	.40	.03	-.69	-1.05			
	s	.97	1.45	.48	.77	.82	.03	.32	.94			
day3	m	.23	-.01	1.31	1.06	.18	.02	-.75	-.90			
	s	.57	.76	.53	.55	.38	.01	.29	.50			
2. Correlation Coefficients (r)												
The values in the upper (lower) triangle are for t1- (q1-)												
D1	D1				D2				D3			
	day1	day2	day3		day1	day2	day3		day1	day2	day3	
		.94	.98	.89		.41	.58	.22		.41	.50	.50
D2	D1				D2				D3			
	day1	day2	day3		day1	day2	day3		day1	day2	day3	
		.51	.69	.55		.32	.44	.03		.32	.44	.50
D3	D1				D2				D3			
	day1	day2	day3		day1	day2	day3		day1	day2	day3	
		.40	.28	.14		.01	.80	.79		.77	.72	.77
D4	D1				D2				D3			
	day1	day2	day3		day1	day2	day3		day1	day2	day3	
		.93	.95	.83		.29	.84	.85		.70	.56	.67
Here,												
D1 = A2 - A1												
D2 = B2 - B1												
D3 = B1 - A1												
D4 = B2 - A2												

Summary Tables of Statistics of Models A1, A2, B1 and B2 at (2,2)												
1. Means (m) and standard Deviations (s)												
	H				E							
	D1	D2	D3	D4	D1	D2	D3	D4				
day1	m	43.3	7.6	51.4	15.6	-49.7	-2.7	-84.6	-37.7			
	s	42.1	50.5	41.3	16.2	29.1	7.6	63.9	52.6			
day2	m	36.4	-17.1	88.5	35.1	-50.6	0.4	-121.6	-70.5			
	s	57.7	60.0	60.9	30.4	38.9	0.9	75.2	69.1			
day3	m	73.9	1.1	106.9	34.1	-81.7	-0.8	-151.8	-70.9			
	s	43.1	31.8	45.8	21.1	38.6	2.0	62.6	46.3			

2. Correlation Coefficients (r)												
The values in the upper (lower) triangle are for H- (E-) correlations.												
D1	D1				D2				D3			
	day1	day2	day3		day1	day2	day3		day1	day2	day3	
		.83	.82	.71		.11	.07	.42		.63	.63	.62
D2	D1				D2				D3			
	day1	day2	day3		day1	day2	day3		day1	day2	day3	
		.10	.34	.44		.53	.39	.67		.18	.18	.88
D3	D1				D2				D3			
	day1	day2	day3		day1	day2	day3		day1	day2	day3	
		.31	.69	.18		.31	.69	.18		.88	.86	.80
D4	D1				D2				D3			
	day1	day2	day3		day1	day2	day3		day1	day2	day3	
		.08	.14	.10		.08	.14	.10		.88	.86	.80
Here,												
D1 = A2 - A1												
D2 = B2 - B1												
D3 = B1 - A1												
D4 = B2 - A2												

Table 11a. Same as in Table 10a, Except for Gridpoint (2,4)

Summary Tables of Statistics of Models A1, A2, B1 and B2 at (2,4)

1. Means (m) and standard Deviations (s)

	t1				q1			
	A1	A2	B1	B2	A1	A2	B1	B2
day1	m	14.33	14.16	15.00	14.96	5.64	6.11	5.25
	s	4.64	5.96	4.55	5.80	0.64	0.56	0.58
day2	m	10.89	10.92	11.71	11.96	3.65	4.10	3.19
	s	4.52	5.48	4.31	5.40	0.60	0.54	0.55
day3	m	6.53	6.94	7.19	7.86	3.60	4.01	3.25
	s	4.17	5.21	4.05	5.19	0.36	0.27	0.29

2. Correlation Coefficients (r)

The values in the upper (lower) triangle are for t1- (q1-)
correlations.

	A1	A2	B1	B2
A1				
	day1	.97	1.00	.98
	day2	.98	1.00	.99
A2				
	day1	.73	.97	1.00
	day2	.91	.98	1.00
B1				
	day1	.95	.63	.98
	day2	.80	.62	.99
B2				
	day1	.90	.67	.98
	day2	.82	.64	.99

Summary Tables of Statistics of Models A1, A2, B1 and B2 at (2,4)

1. Means (m) and standard Deviations (s)

	H				E			
	A1	A2	B1	B2	A1	A2	B1	B2
day1	m	-45.3	-25.9	-9.5	-4.8	64.8	49.5	12.8
	s	118.4	76.2	112.0	69.6	16.8	22.8	16.0
day2	m	-11.1	1.4	36.6	29.8	67.5	54.2	2.6
	s	130.5	92.7	131.9	95.4	2.9	16.8	2.1
day3	m	17.3	17.7	64.3	46.2	63.4	53.5	1.5
	s	132.2	67.6	131.8	92.6	8.6	20.7	0.7

2. Correlation Coefficients (r)

The values in the upper (lower) triangle are for H- (E-)
correlations.

	A1	A2	B1	B2
A1				
	day1	.99	1.00	1.00
	day2	.99	1.00	1.00
A2				
	day1	.85	.98	.99
	day2	.64	.99	.99
B1				
	day1	.53	.36	1.00
	day2	.55	.53	1.00
B2				
	day1	.57	.43	.99
	day2	.60	.76	.82

Table 11b. Same as in Table 10b, Except for Gridpoint (2,4)

Summary Tables of Statistics of Models A1, A2, B1 and B2 at (2,4)									
1. Means (m) and standard Deviations (s)									
	t1				q1				
	D1	D2	D3	D4	D1	D2	D3	D4	
m	-.17	-.05	.67	.80	.48	.10	-.39	-.76	
day1	s 1.78	1.65	.24	.46	.44	.13	.20	.47	
day2	m .03	.25	.82	1.04	.46	.03	-.49	-.92	
day2	s 1.34	1.36	.39	.30	.25	.02	.36	.46	
day3	m .40	.68	.65	.92	.41	.02	-.35	-.74	
day3	s 1.52	1.47	.16	.33	.26	.01	.09	.21	

Summary Tables of Statistics of Models A1, A2, B1 and B2 at (2,4)									
1. Means (m) and standard Deviations (s)									
	H				E				
	D1	D2	D3	D4	D1	D2	D3	D4	
m	19.4	4.7	35.8	21.1	-15.4	-3.6	-52.1	-40.3	
day1	s 44.3	43.2	13.1	12.0	12.3	4.7	16.0	20.7	
day2	m 12.5	-6.8	47.7	28.4	-13.3	-0.0	-64.9	-51.6	
day2	s 39.9	37.1	6.5	11.0	15.1	1.2	2.4	15.6	
day3	m 0.4	-18.1	47.0	28.5	-9.9	0.2	-61.9	-51.8	
day3	s 41.8	39.4	8.0	11.3	14.7	0.5	8.2	20.0	

2. Correlation Coefficients (r)									
The values in the upper (lower) triangle are for H- (E-) correlations.									
	D1				D2				
	day1	day2	day3	day4	day1	day2	day3	day4	
D1									
D2	.52				.22				
D2	.54	.52			.12				
D2	.54	.54	.52		.45	.34			
D3	.04	.29	.63		.28	.55			
D3	.20	.78	.57	.63	.20	.36			
D3	.63	.57	.57	.63	.52	.22			
D4	.82	.09	.67	.94	.76	.33	.81		
D4	.67	.85	.85	.94	.99	.10	.32		
D4	.94	.38	.38	.94	.94	.40	.78		

Here,	D1 = A2 - A1
	D2 = B2 - B1
	D3 = B1 - A1
	D4 = B2 - A2

Here,	D1 = A2 - A1
	D2 = B2 - B1
	D3 = B1 - A1
	D4 = B2 - A2

Table 12a. Same as in Table 10a, Except for Gridpoint (7,2)

Summary Tables of Statistics of Models A1, A2, B1 and B2 at (7,2)									
1. Means (m) and standard Deviations (s)									
	t1			q1			H		
	A1	A2	B1	B2	A1	A2	B1	A1	A2
m	8.91	9.12	8.91	9.14	7.43	7.73	7.44	11.0	11.5
day1	s	1.41	1.38	1.40	1.37	0.70	0.70	11.2	12.8
m	13.06	13.35	13.01	13.32	9.61	10.17	9.67	18.8	19.6
day2	s	1.53	1.82	1.48	1.73	0.72	0.75	32.7	32.8
m	2.78	3.20	2.79	3.29	4.74	5.04	4.79	-15.8	-19.5
day3	s	4.56	4.78	4.54	4.75	1.62	1.72	56.2	47.5
								24.1	24.1
								89.3	66.8
								198.7	106.2
								176.7	99.8
								96.9	191.9
2. Correlation Coefficients (r)									
The values in the upper (lower) triangle are for t1- (q1-) correlations.									
	A1			A2			B1		
	A1	A2	B1	B2	A1	A2	B1	A2	B2
day1									
day2		.99	1.00	.99					
day3		.97	1.00	.98					
A1		1.00	1.00	1.00					
day1									
day2		.92	.98	1.00					
day3		.67	.95	1.00					
A2		.99	.99	1.00					
day1									
day2		1.00	.92	.99					
day3		1.00	.72	.99					
B1									
day1									
day2									
day3									
B2									
day1									
day2									
day3									

Table 12b. Same as in Table 10b, Except for Gridpoint (7,2)

Summary Tables of Statistics of Models A1, A2, B1 and B2 at (7,2)									
1. Means (m) and standard Deviations (s)									
	t1				q1				
	D1	D2	D3	D4	D1	D2	D3	D4	
day1	m	.21	.23	-.00	.02	.30	.11	.01	-.18
	s	.22	.22	.01	.08	.27	.11	.03	.18
day2	m	.29	.30	-.05	-.03	.56	.21	.06	-.29
	s	.51	.49	.11	.14	.93	.32	.08	.59
day3	m	.42	.50	.01	.08	.30	.19	.05	-.06
	s	.45	.41	.30	.27	.26	.17	.06	.13
2. Correlation Coefficients (r)									
The values in the upper (lower) triangle are for t1- (q1-) correlations.									
	D1	D2	D3	D4	D1	D2	D3	D4	
D1	day1	.99	-.39	-.24	day1	.91	-.27	-.41	D4
	day2	1.00	-.96	-.93	day2	.89	.62	.47	D3
	day3	.99	-.03	-.18	day3	1.00	-.31	-.31	D2
D2	day1	.95	-.26	-.09	day1	.91	-.27	-.41	D4
	day2	.93	-.95	-.91	day2	.89	.62	.47	D3
	day3	.95	-.13	-.26	day3	1.00	-.31	-.31	D2
D3	day1	-.08	.14	.97	day1	.91	-.27	-.41	D4
	day2	.84	.90	.96	day2	.89	.62	.47	D3
	day3	.34	.61	.98	day3	1.00	-.31	-.31	D2
D4	day1	-.95	-.82	.35	day1	.91	-.27	-.41	D4
	day2	-.97	-.81	-.70	day2	.89	.62	.47	D3
	day3	-.53	-.24	.60	day3	1.00	-.31	-.31	D2
Here,									
D1 = A2 - A1									
D2 = B2 - B1									
D3 = B1 - A1									
D4 = B2 - A2									

Table 13a. Same as in Table 10a, Except for Gridpoint (7,4)

Summary Tables of Statistics of Models A1, A2, B1 and B2 at (7,4)									
1. Means (m) and standard Deviations (s)									
	t1			q1			H		
	A1	A2	B1	B2	A1	A2	B1	B2	E
m	19.00	19.12	18.99	19.12	13.68	13.94	13.68	13.79	
day1									
s	0.89	0.95	0.90	0.99	0.78	0.97	0.78	0.85	
m	18.42	18.58	18.38	18.56	12.75	13.00	12.81	13.02	
day2									
s	1.12	1.45	1.04	1.41	0.64	1.15	0.66	0.96	
m	12.87	13.49	13.77	14.14	8.15	8.49	7.65	7.84	
day3									
s	3.97	4.47	3.78	4.38	2.44	2.76	2.63	2.77	
2. Correlation Coefficients (r)									
The values in the upper (lower) triangle are for t1- (q1-)									
	A1			A2			B1		
	A1	A2	B1	A1	A2	B1	A1	A2	B2
day1									
day2									
day3									
A1									
A2									
B1									
B2									

Summary Tables of Statistics of Models A1, A2, B1 and B2 at (7,4)									
1. Means (m) and standard Deviations (s)									
	H			E			B1		
	A1	A2	B1	A1	A2	B1	A1	A2	B2
m	-13.3	-0.5	-14.9	-0.2	73.1	48.8	73.1	48.8	35.4
day1									
s	45.5	19.2	43.6	19.1	69.2	54.0	70.8	51.3	38.3
day2									
m	-12.1	2.1	-16.8	1.8	78.4	51.9	89.5	51.3	71.1
day3									
s	31.0	21.7	24.2	20.9	101.5	83.5	113.1	52.0	39.2
m	-70.6	4.0	56.4	36.0	229.4	114.4	52.0	39.2	50.9
day3									
s	134.6	74.5	132.0	79.2	118.7	85.8	74.5	50.9	
2. Correlation Coefficients (r)									
The values in the upper (lower) triangle are for H- (E-) correlations.									
	A1			A2			B1		
	A1	A2	B1	A1	A2	B1	A1	A2	B2
day1									
day2									
day3									
A1									
A2									
B1									
B2									

Another noteworthy feature found in part a is the difference between t_1 and q_1 on one hand and H and E on the other of diurnal variations of the individual variables. In other words, it shows that the diurnal ranges of H and E relative to their respective daily means are much greater than those of t_1 and q_1 . It signifies the fact that the thermodynamic state of the surface as represented by t_1 and q_1 is kept relatively stable by a balance of energy fluxes of large fluctuations.

The statistics of four differences among the models in part b measure degrees of coherence in the impacts of a change in one attribute between the old and new versions of the other attribute. As expected, good correlation in the differences are found, when it exists, only between the related pairs, for example, between D1: the difference in output between A1 and B1, and D4: between A2 and B2. It is also quite obvious that there is little uniformity in the statistics of differences of effects of changes among the four gridpoints; suggesting that effects of the changes are very much dependent on circumstances. The figures in these tables make obvious the futility of any effort to find some quantitative statistical relationship between the model changes and their impacts on surface parameters that is independent of either time and space. Yet, there are some features that cannot help but draw our attention; for example, the strong similarity in the pattern of statistics of D3 and D4 for not only t_1 and q_1 but also H and E between two grid points in the west and, an equally strong similarity but different in pattern, of the statistics in D1 and D2 for t_1 and q_1 .

A further comparison is made directly with time series of the surface parameters put side by side from a pair of comparable models, such as those shown in Figures 9-12. Each frame in any figure of the group contains time series of a surface variable from a pair of the models, A1, A2, B1, and B2 at one of the four gridpoints, (2,2), (2,4), (7,2), and (7,4), during Jan 12, 12 UTC to Jan 15, 12 UTC of 1979.

Figures 9 and 10 illustrate the impacts on surface temperature and on sensible heat flux, respectively, of the change in form, that is, exchange-coefficient formulas, and Figures 11 and 12 the impacts on the same variables by the change in algorithm for surface-energy balance. Part A in each is in the west: at gridpoints (2,2) and (2,4) and part B is in the east: at gridpoints (7,2) and (7,4).

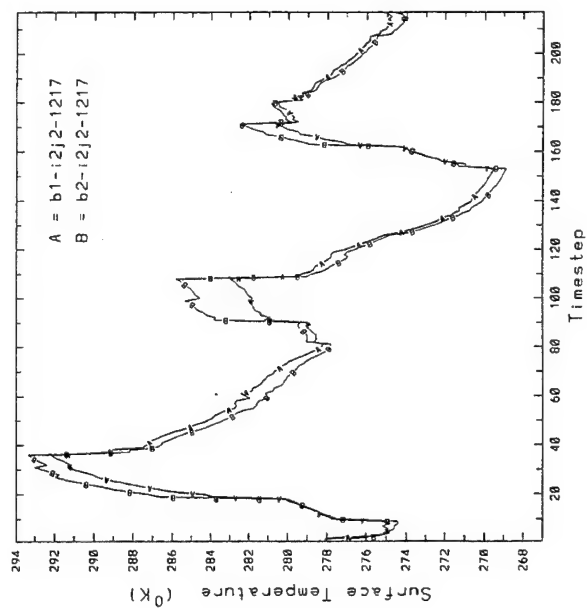
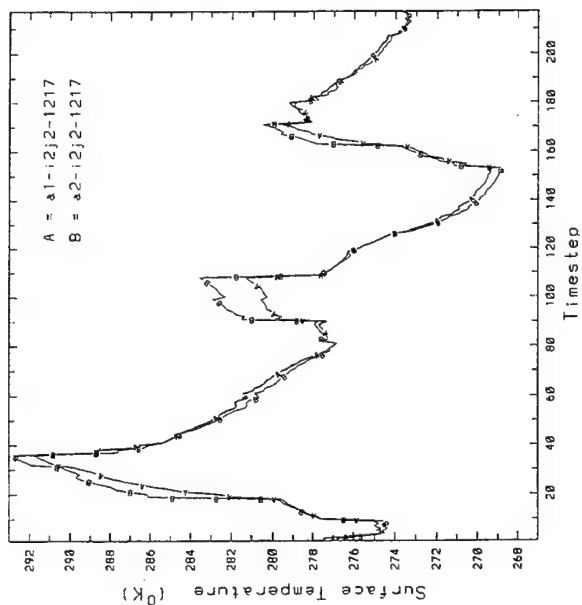
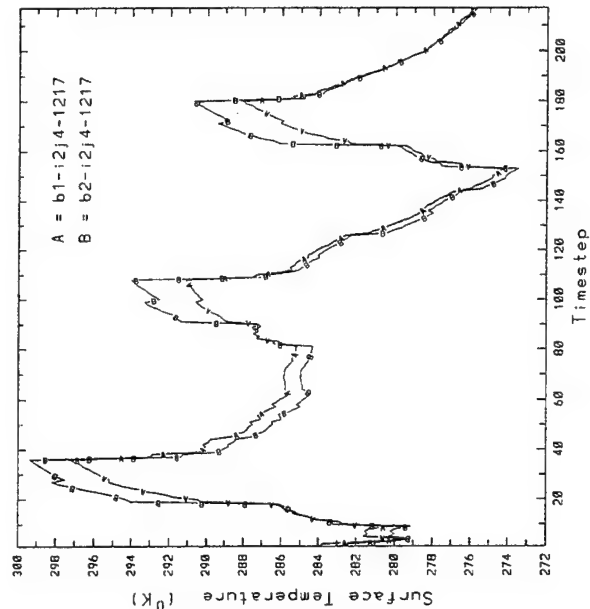
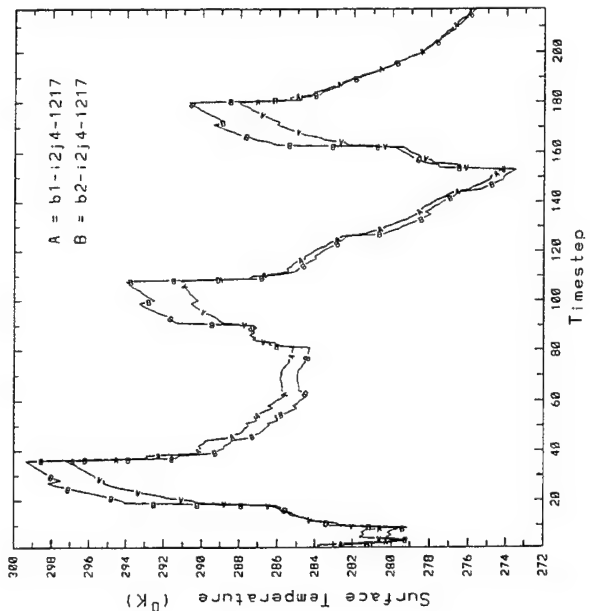


Figure 9A. Pairwise Comparisons of Surface Temperatures Between the Old and New Exchange Coefficients at Gridpoints (2,2) and 2,4)

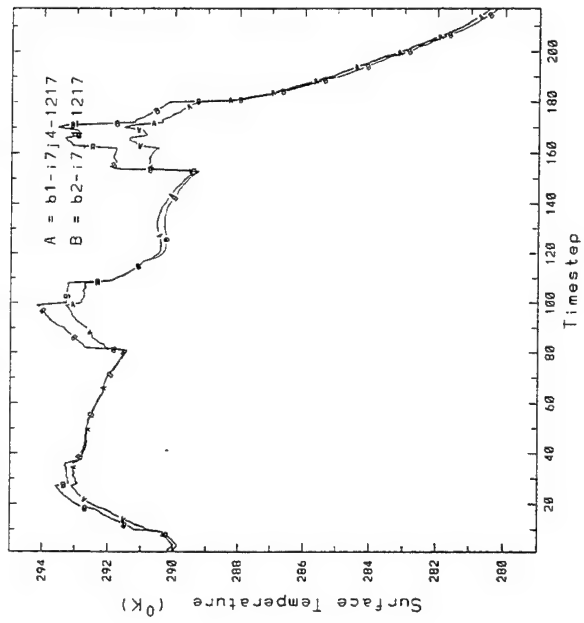
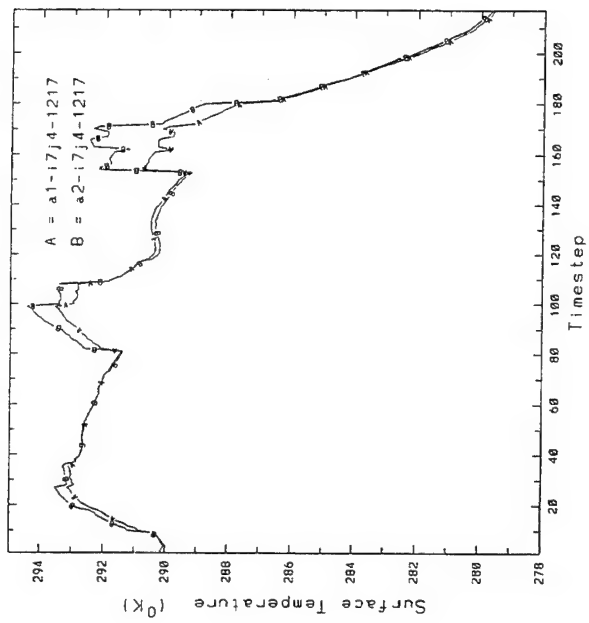
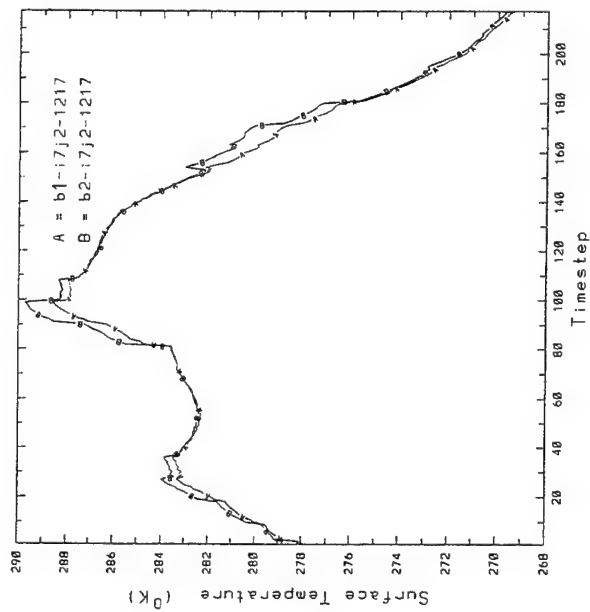
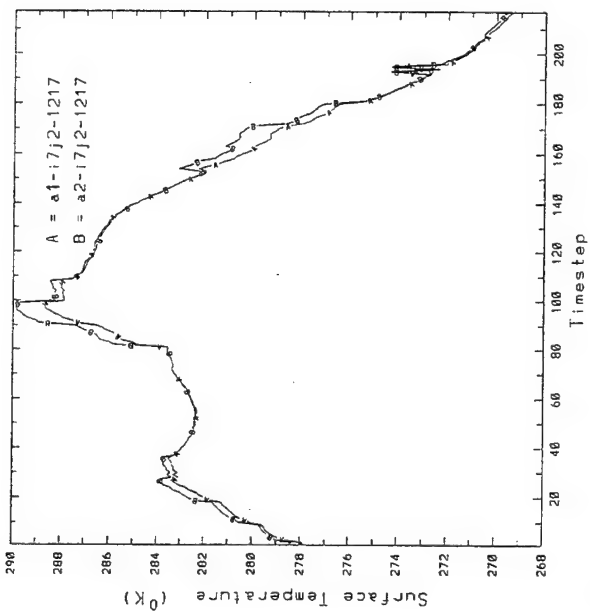


Figure 9B. Same as in Figure 9A, Except for Gridpoints (7,2) and (7,4)

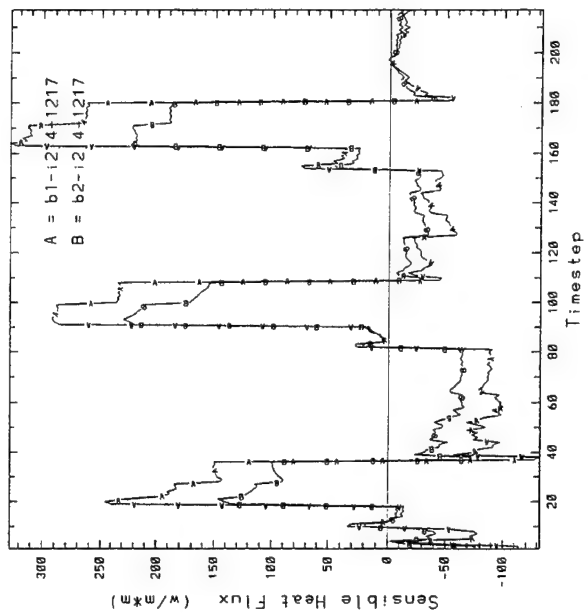
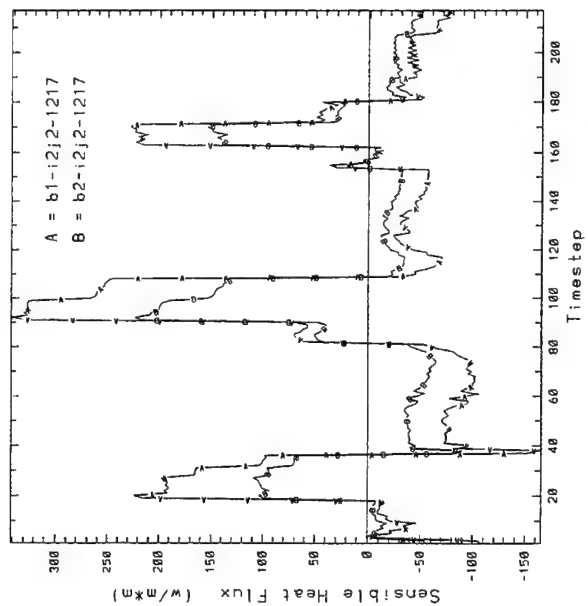
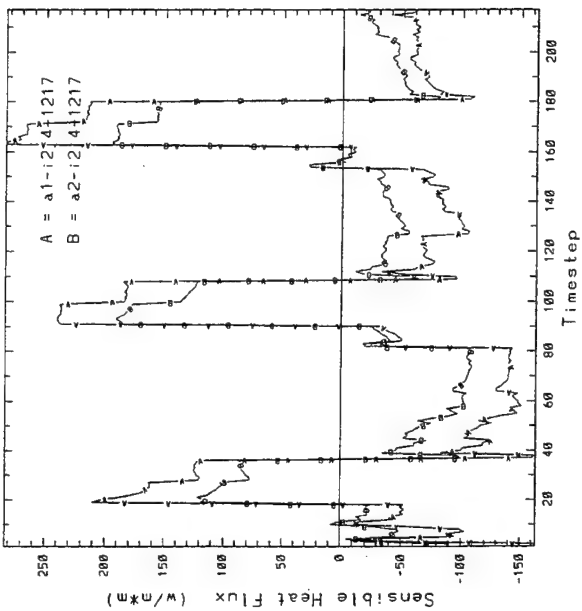
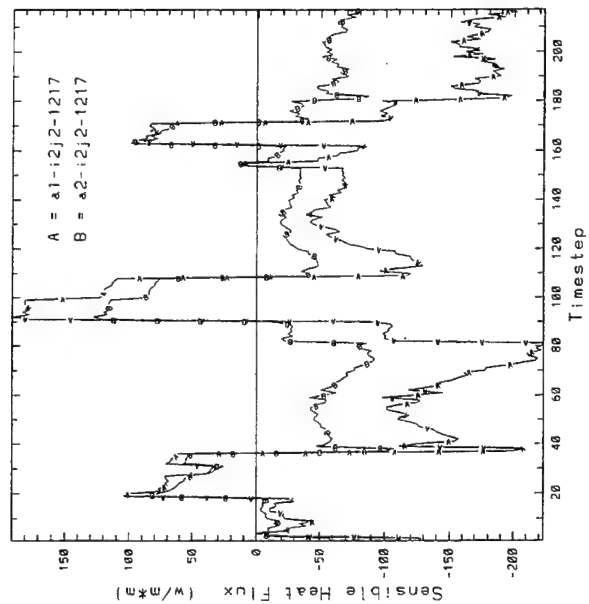


Figure 10A. Pairwise Comparisons of Sensible Heat Fluxes Between the Old and New Exchange Coefficients at Gridpoints (2,2) and (2,4)

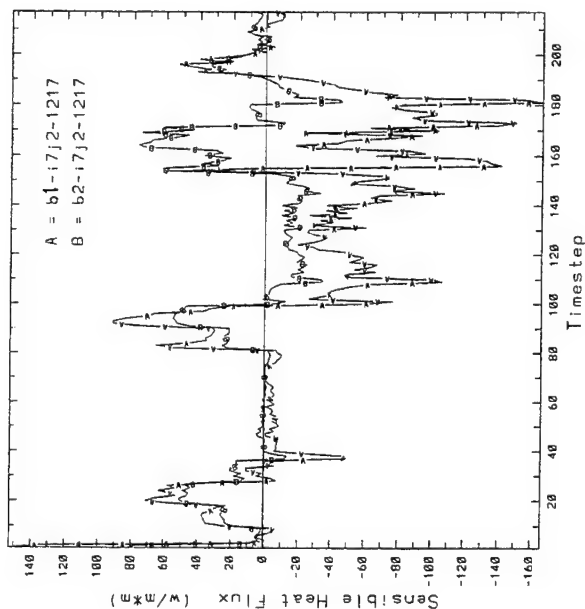
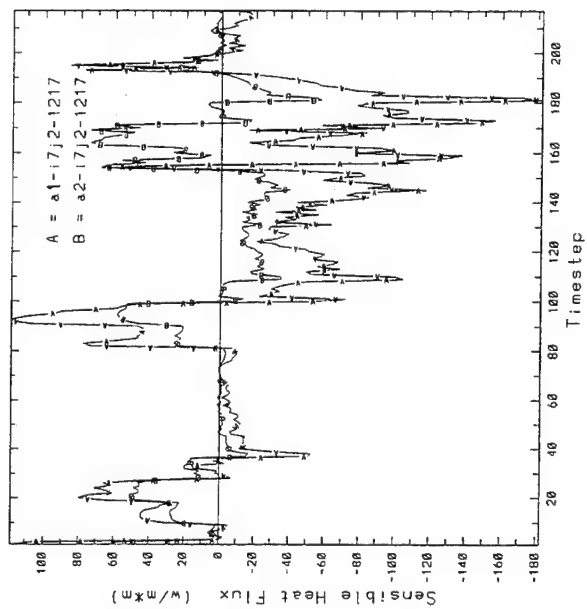
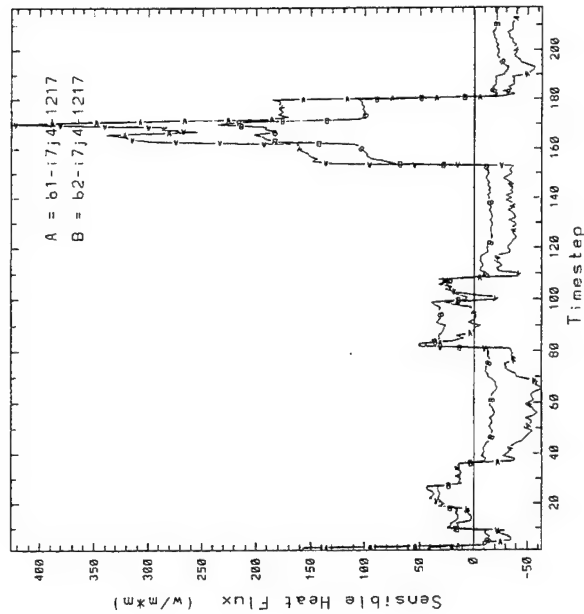
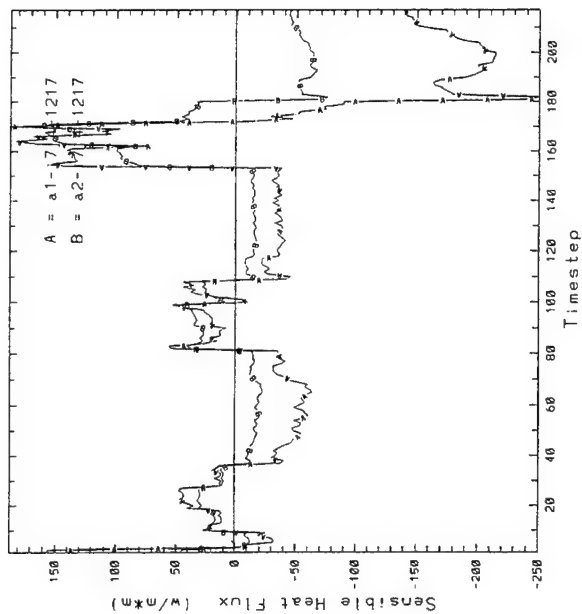


Figure 10B. Same as in Figure 10A, Except for Gridpoints (7,2) and (7,4)

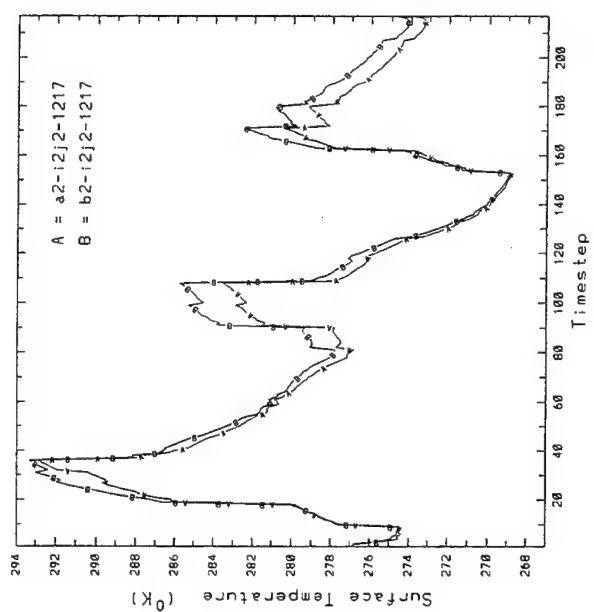
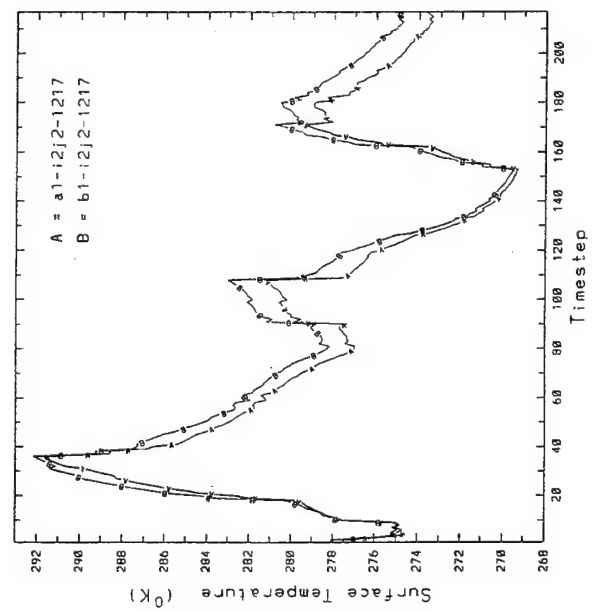
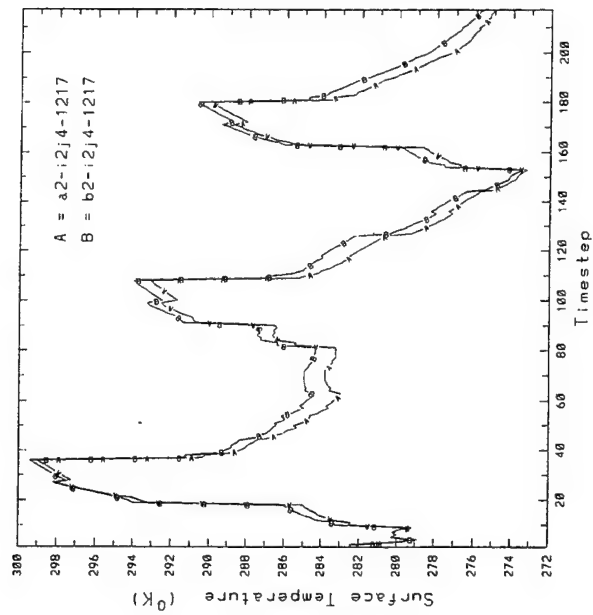
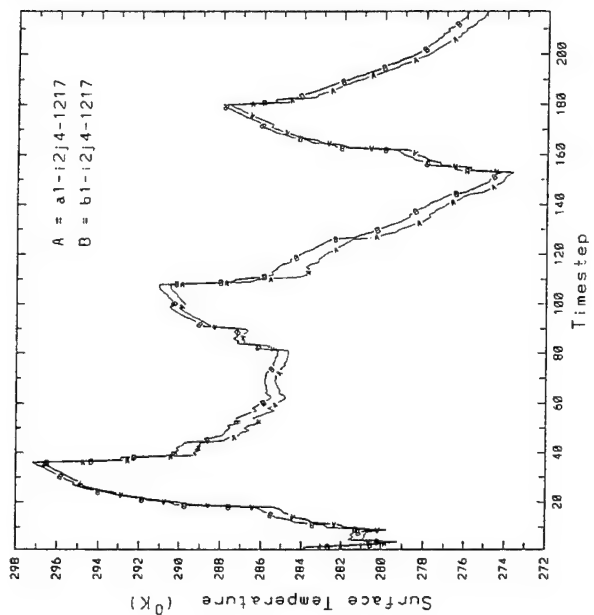


Figure 11A. Pairwise Comparisons of Surface Temperatures Between the Old and New Algorithms at Gridpoints (2,2) and (2,4)

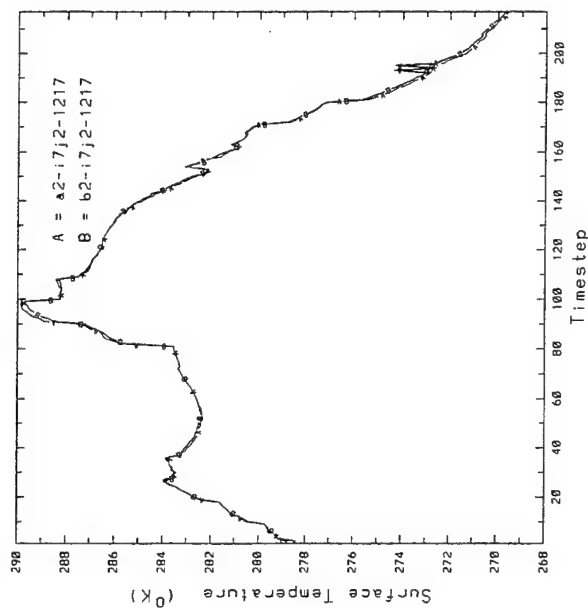
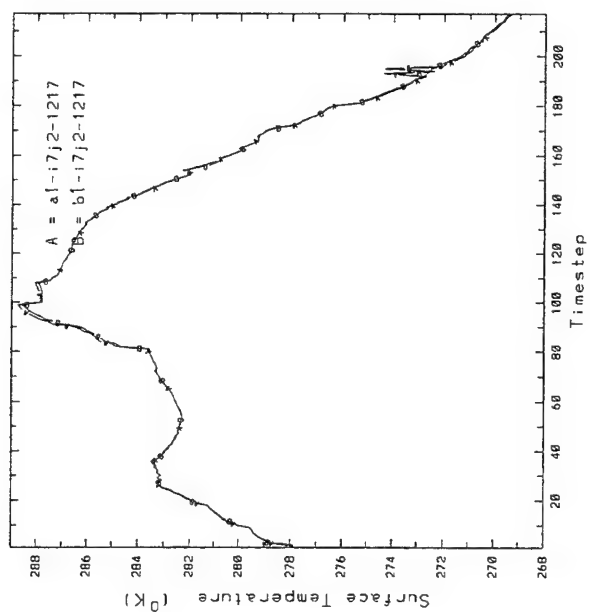
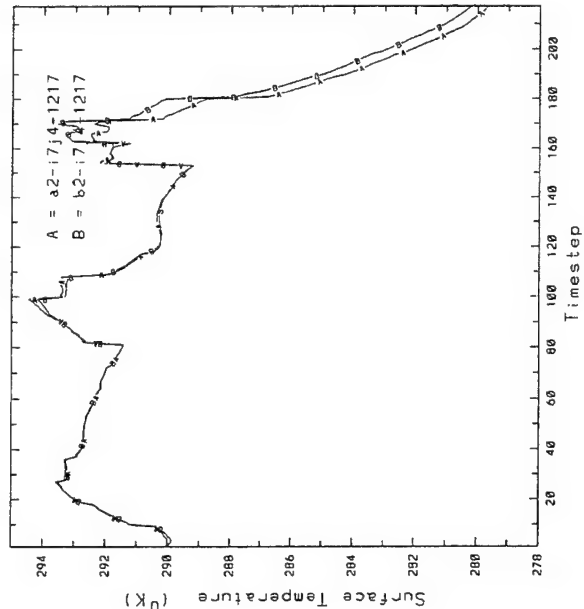
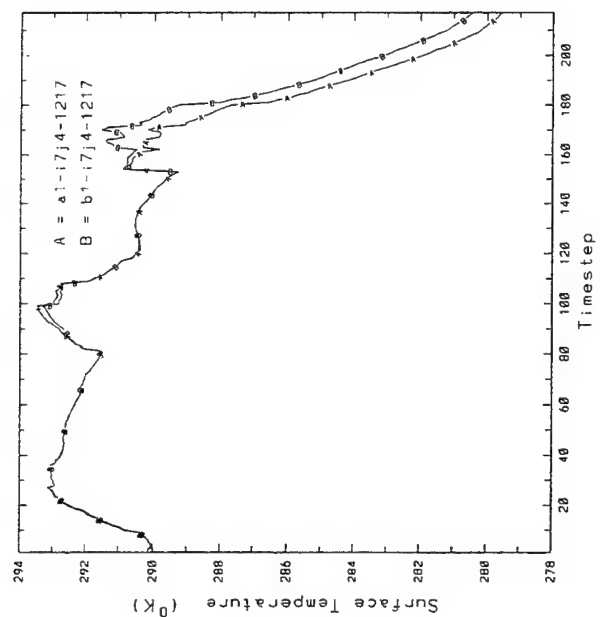


Figure 11B. Same as in Figure 11A, Except for Gridpoints (7,2) and (7,4)

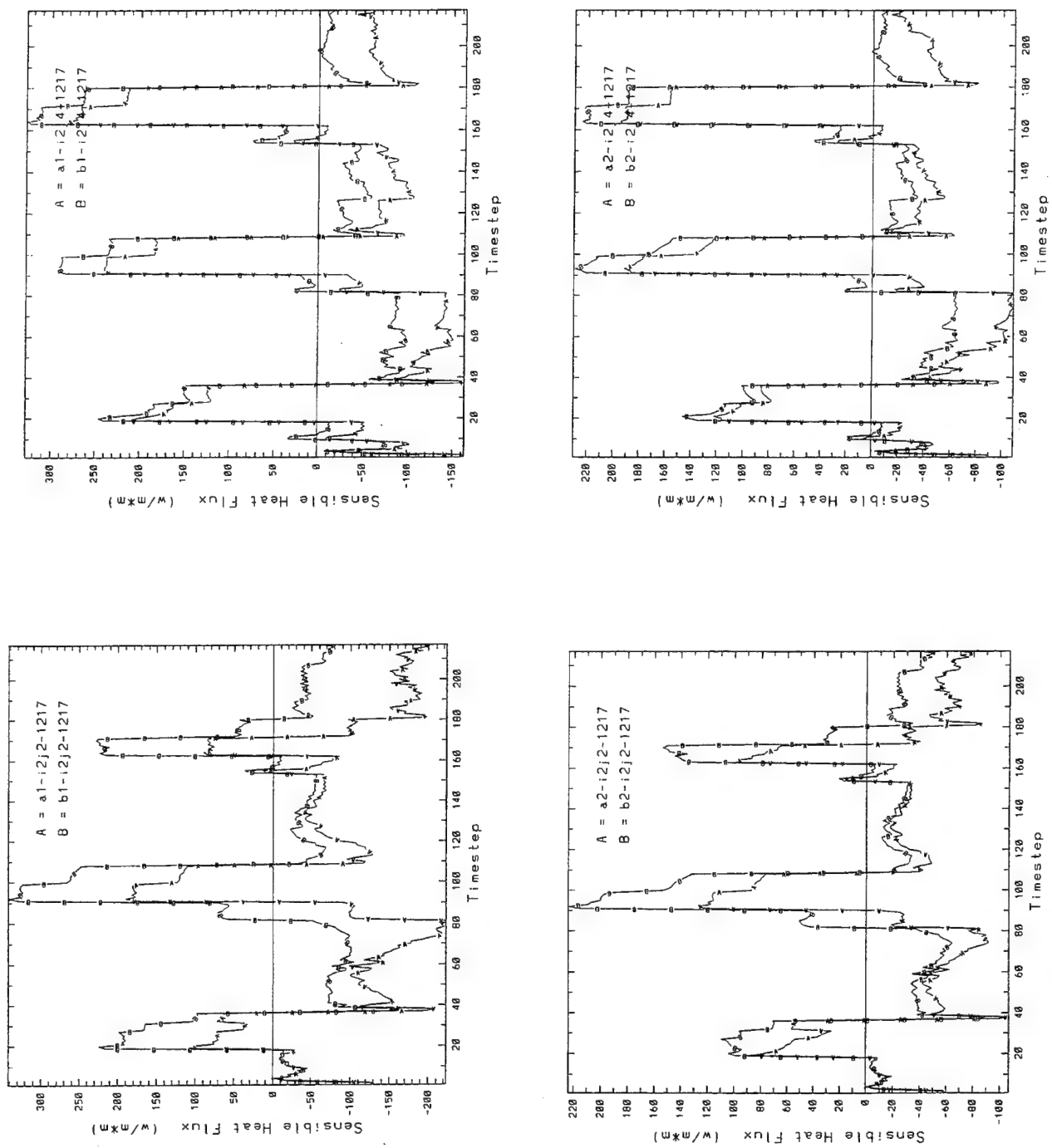


Figure 12A. Pairwise Comparisons of Sensible Heat Fluxes Between the Old and New Algorithms at Gridpoints (2,2) and (2,4)

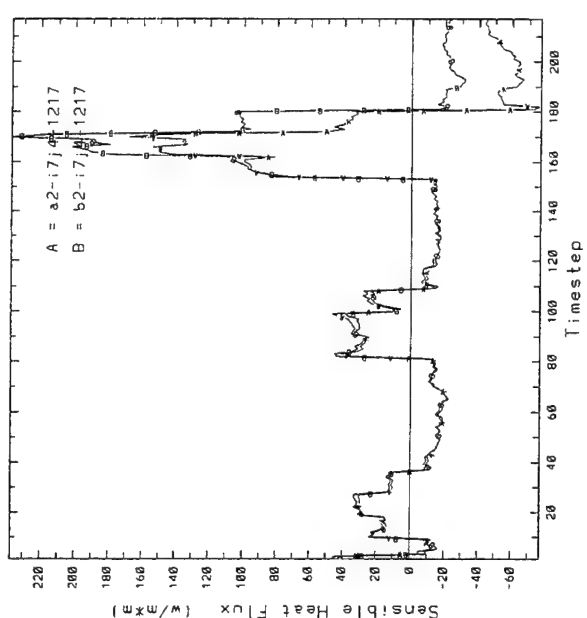
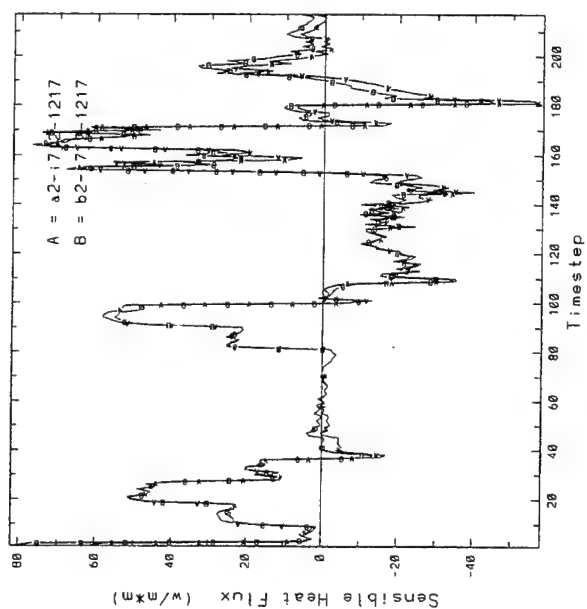
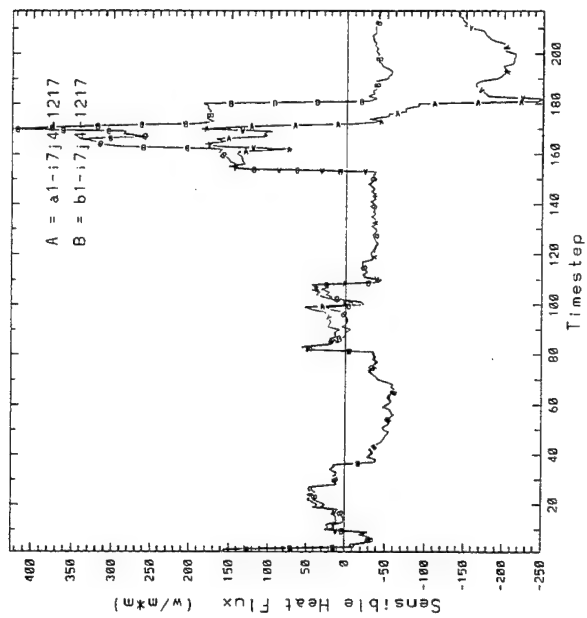
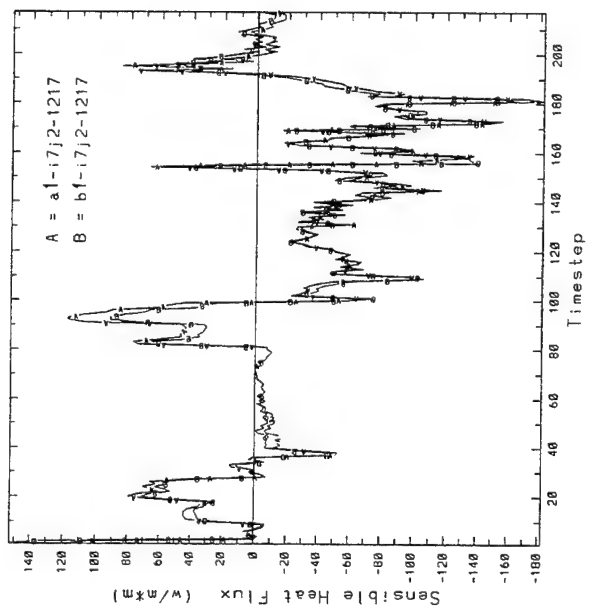


Figure 12B. Same as in Figure 12A, Except for Gridpoints (7,2) and (7,4)

The analysis of the surface-layer exchange-coefficient formulas presented earlier (Section 2.1) showed that, when everything else remains the same, the change in formulas from old to new reduces the rates of exchange of heat and moisture between the earth and the atmosphere. We may take a first guess at the subsequent effect on surface parameters by considering the equation for surface energy balance with neither precipitation nor snow cover. It is given by (see Eq. (36)),

$$FD = H + E + G + FU.$$

With the downward radiative flux, $FD > 0$ always, a reduced sum of H and E requires an increased sum of G , ground heat flux, and FU , upward radiative flux; which is realized by a surface temperature that is warmer by day and colder at night. Such a deduction is qualitative and an approximation to the extent that it presumes no reversal in any of the gradients within the immediate layers surrounding the surface. Quantitative relationships between temperature or specific humidity at the surface and surface fluxes depend upon other factors such as wind speed, thermal and moisture gradients and thermal stability in the surface layer.

Figures 9 and 10 together provide a good example of the scenario described above, particularly in part A where diurnal variations of both the temperature and the flux and the relation between the temperature and the flux are both well defined. The same is found in most of part B, though more muted, except on the third day (timestep beyond 144) at gridpoint (7,2) in daytime when both algorithms show changes in thermal gradient between the old and new formulas.

We also note in these figures that while the difference in algorithm appears to affect the impacts on the temperature only slightly, there are more differences in the impacts on the sensible heat flux, especially in the west and in the third night at gridpoint (7,4). It is also apparent that the temperature-flux relationship depends much on ancillary conditions as well as on the model structure.

Time-series plots such as Figures 9-12 not only provide new information not present in summary statistics such as those of Tables 10-13, but also furnish new insights into them: for example, that the daily means are often small differences of two large but opposite quantities and that the daily standard deviation tells more of model

characteristics than the corresponding daily mean of a parameter. They also point out a subtle difference in the statistics of differences between the temperature and the flux. In temperature, the differences are opposite in sign between day and night, while in flux, they are mostly of one sign both day and night.

The two moisture-related parameters, surface specific humidity, q_1 , and evaporative latent heat flux, E , exhibit (not shown) diurnal cycles similar to those for temperature and sensitive heat flux, but with some variations in the differences of impacts between the models and between gridpoints in the west and those in the east. These variations may be most likely ascribed to the intrinsic differences between thermal and hydrological distributions in the environment. For instance, rarely were there timesteps at which q_1 was lower than the specific humidity at the level above in all gridpoints; E was thus almost always nonnegative and even when E was negative, its magnitude turned out to be very small. The new formulas reduce E and increase q_1 with a few exceptions at night when the differences are small, more in daytime than at night and more in the east than west.

The third of the surface fluxes, ground heat flux, G , directs away or toward the surface as the thermal gradient in the top soil layer points down or up in the vertical. Thus, it too has a typical diurnal cycle in which the flux changes direction; positive (downward) by day and negative (upward) by night, as H does. In most cases, however, unlike H , the new formulas of exchange coefficient produced greater magnitudes both day and night irrespective of algorithm and location. Naturally, as in the other fluxes, the coherence in the differences due to the change in formulas between the two algorithms varies from day to day and from gridpoint to gridpoint, as indicated by the values of correlation coefficient between $D1$ and $D2$ in part b of Tables 6-9.

We next turn to Figures 11 and 12, which present the impacts from the change in algorithm. We noted earlier that the new algorithm appeared to produce reasonable values in all surface parameters in cases of precipitation on snow-covered surfaces where the old algorithm clearly failed. Other than that, unlike the change in formulas of exchange-coefficient, we had little indication of what to expect from installing the

collection of changes described in Section 3.

We now find in these figures that the new algorithm increases both surface temperature and sensible heat flux in the west both day and night, regardless of the formula for exchange coefficient, but causes little change in the east except for the third day at gridpoint (7,4). This pattern of contrast in the impacts between the west and east--1 K in t_1 and 50 $\text{w/m}^2\text{m}$ in H in the west and one-tenth of that or less in the east--is even well-reflected in the daily statistics of differences, D3 and D4. Similar contrasts are also found in q_1 , E and G , though not as stark as those of t_1 or H . Having found no obvious cause of the contrast in the synoptic data directly available, we think it to be the result of a happenstance in the east where the surface temperatures in the two algorithms turned out not only to be close to each other, but also close to the temperature above.

With regard to differences in flux due to the change in algorithm, G is biased the same way as H , that is, the new algorithm increases it at all times. q_1 and E , however, exhibit the opposite biases to those of t_1 and H , respectively. The new algorithm produces far less, but still positive, evaporative latent heat flux, accompanied by lower specific humidity than the old at all times. These t_1 - H and q_1 - E relationships found in differences of impact are opposite to those found with the change in formulas. The apparent contradiction, however, is not really a contradiction but rather to be expected on account of the difference in cause. Earlier, with the change in formulas, the immediate culprit in changing the flux values was the exchange coefficient, but now with the change in algorithm it is the surface temperature or specific humidity that affects the corresponding flux value. Thus, in estimating the impact on fluxes of the change in algorithm, the first approximation should be made based on Eqs. (26)-(28).

We have demonstrated that although both the change in formulas and the change in algorithm are minor perturbations and their impacts can often be accounted for by linear approximations, magnitudes of the impact can be significant even on a daily basis. The regression relations are highly dependent upon ancillary conditions of environment and model structure. In the limited cases of samples we studied, we have seen that the new formulas of surface-layer exchange coefficient produce larger diurnal

amplitudes in surface temperature and humidity, but smaller fluxes of sensible heat and latent heat of evaporation. The magnitudes of change, however, vary from day to day and from gridpoint to gridpoint and with the change in algorithm. Similar variabilities are found also in the impact of the change in algorithm of seeking surface-energy balance where the new algorithm is seen to increase both surface temperature and sensible heat flux while decreasing humidity and evaporative latent heat flux.

We present Figure 13 for sensible-heat flux and Figure 14 for evaporative latent heat flux to illustrate the impacts on the atmosphere of introducing both changes in the GSM. With reference to these and other figures not shown here, as well as the tables of statistics such as Tables 10-13, we may qualitatively summarize the impacts of including both changes on the surface variables as follows:

Surface temperature rises and specific humidity decreases with the combined effect of reducing the surface relative humidity. Sensible heat flux increases and evaporative latent heat flux decreases, with both fluxes having smaller amplitudes in their diurnal cycles. The differences due to the changes are greater with larger diurnal variations in synoptic conditions. Measured by daily averages, the changes in surface temperature and specific humidity are small but changes in the fluxes are generally significantly large in comparison with their absolute values.

4.3 Methods of Solving Energy-Balance Equations

Effects on surface outputs by the method chosen for solving the equations of surface energy balance are examined by comparing values of individual fluxes at the surface among three methods:

- (1) solving the linearized equations without iteration,
- (2) solving the linearized equations with iteration to account for adjustments in the parameters that depend on the surface variables, and,
- (3) solving the nonlinear balance equations with iteration.

In method (2), iteration ends when none of four fluxes, namely, sensible heat (H), ground heat (G), evaporative latent heat (E) and upward radiative heat (FU), nor the

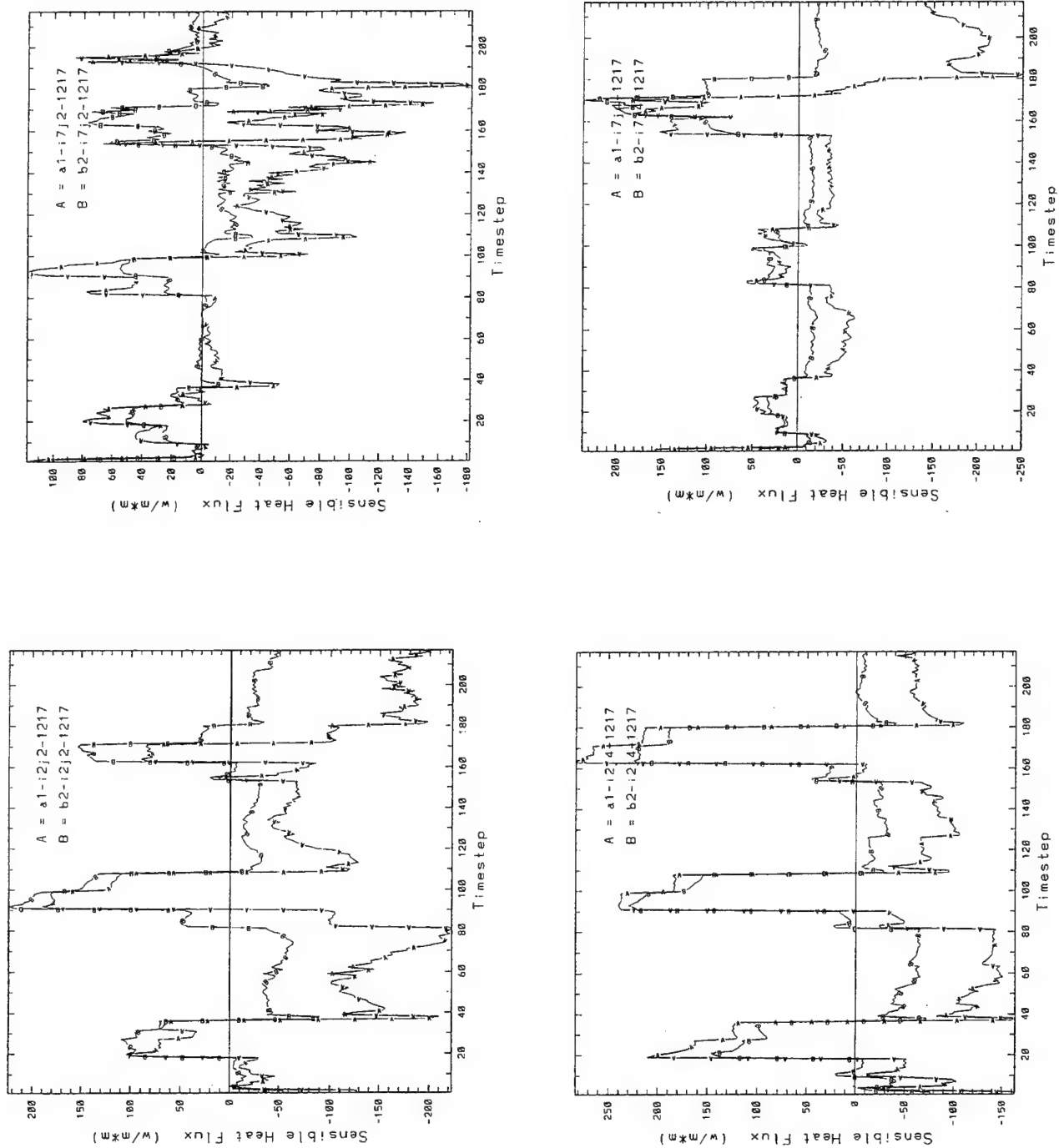


Figure 13. Comparisons of Sensible Heat Fluxes Between the Old (A1) and New (B2) Models at Gridpoints (2,2), (2,4), (7,2), and (7,4)

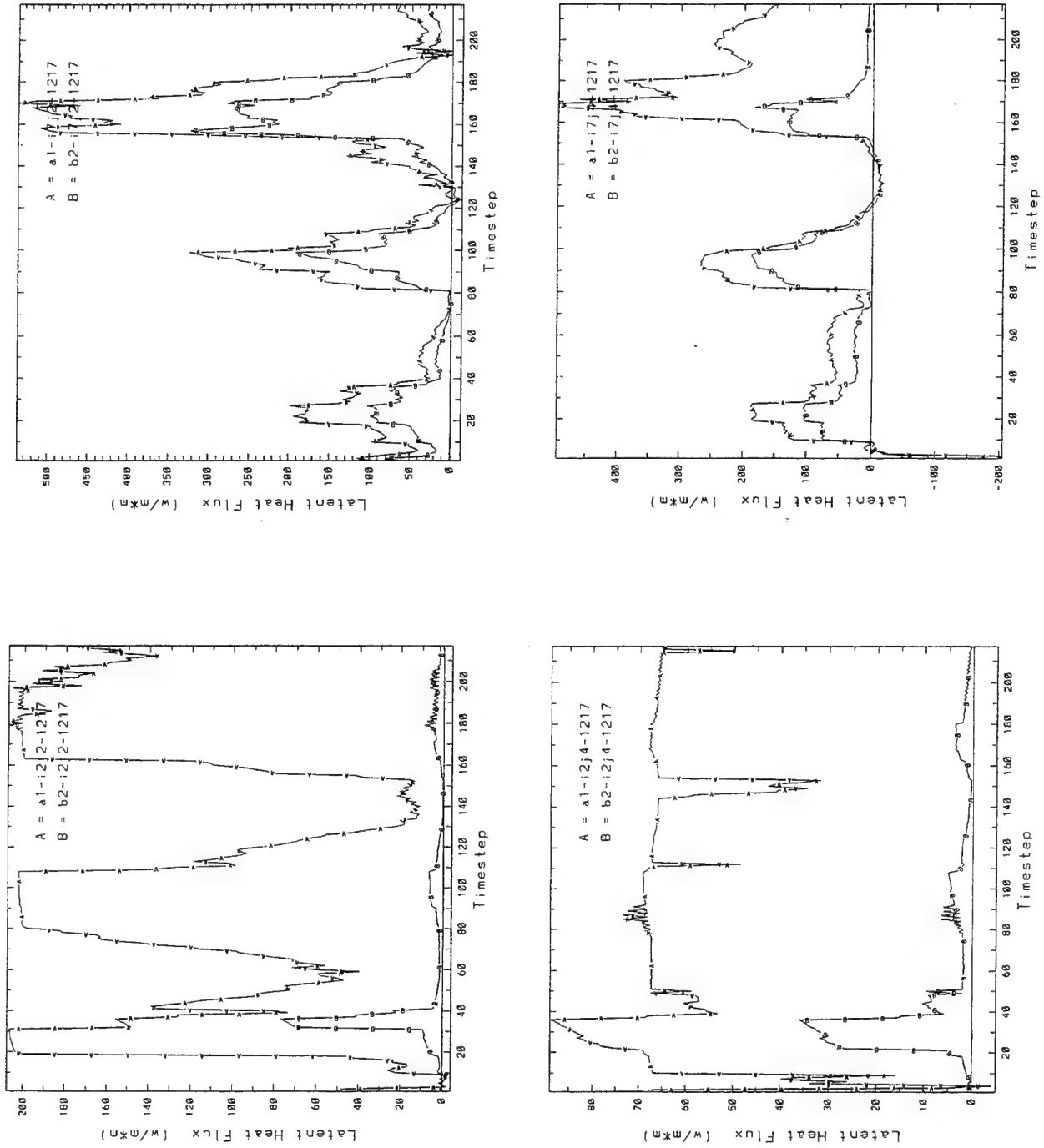


Figure 14. Comparisons of Evaporative Latent Heat Fluxes Between the Old (A1) and New (B2) Models at Gridpoints (2,2), (2,4), (7,2), and (7,4)

balance (B) changes by more than a prescribed threshold value, which has been set at 1 W m^{-2} . In method (3), on the other hand, iteration continues until either the magnitude of the balance becomes less than the threshold value or none of three fluxes, H, G, and E, changes by more than the threshold value between succeeding steps.

Tables 14 and 15 present samples of such results. In each table, on each time step specified in the first column (ns) are four models: A2 that solves the linearized balance equations using the old algorithm and without iteration, B20 and B2 that both solve the linearized balance equation using the new algorithm, but B20 without and B2 with iteration and, C2 that solves the equations nonlinearly with iteration. The third column, under heading 'm', gives the number of iteration steps. The fourth column, under heading 'FD', shows the values of downward radiative flux, which are an output from a subprogram that calculates the radiative transfer within the atmosphere. The next to last column, under heading 'S', presents the net values of three fluxes of heat of phase change, that is, wp, wc, and wm, and the last column gives the balance, that is, the difference between the sum of the outgoing fluxes and the incoming flux, FD. Table 14 is the result at gridpoint (2,2) and Table 15 the result at gridpoint (7,4).

The values from model A2 are included here to indicate the significance of the differences among the other three models. We have drawn the following inferences from these and other similar tables at other locations within the region of the study:

1. The changes in the surface outputs caused by differences in the method of solution are far smaller than that produced with the change in formulas for the exchange coefficient.

2. Iteration does not necessarily reduce the balance when the balance equations are linearized. Generally speaking, iterated solutions of the linearized equations come closer to the iterated solutions of the full or nonlinear balance equations, but there are few exceptions to this general rule and the improvement is at most a few percent of the flux value itself.

3. The nonlinear iterative method obtains individual flux values that meet the specified threshold criteria within a reasonable number of steps and may be considered

14. A Comparison of Surface Energy Fluxes Obtained with Different Methods of Solving the Surface Energy Balance, at Gridpoint (2,2)

Gridpoint (2,2)										Gridpoint (2,2)									
ns	model	m	FD	H	G	E	FU	S	B	ns	model	m	FD	H	G	E	FU	S	B
1	A2	0	244.78	-58.35	-30.81	1.40	332.80	.00	.26	55	A2	0	237.52	-43.19	-78.97	4.71	355.27	.00	.31
	B20	0		-57.18	-31.69	.75	333.20	.00	.30		B20	0		-38.47	-82.82	1.52	357.58	.00	.29
	B2	3		-54.32	-34.17	.72	332.86	.00	.31		B2	3		-35.17	-85.64	1.45	357.18	.00	.31
	C2	5		-54.42	-34.49	.86	332.82	.00	.01		C2	4		-35.23	-86.00	1.61	357.13	.00	.01
9	A2	0	244.78	-19.62	-47.31	-9.70	321.77	.00	.36	63	A2	0	237.52	-56.17	-65.06	8.66	350.33	.00	.25
	B20	0		-19.55	-53.95	-3.22	321.92	.00	.42		B20	0		-50.15	-65.94	1.48	352.37	.00	.24
	B2	3		-17.28	-56.08	-3.06	321.64	.00	.43		B2	2		-47.44	-68.27	1.44	352.04	.00	.25
	C2	6		-17.49	-57.82	-1.32	321.41	.00	.00		C2	4		-47.53	-68.55	1.59	352.00	.00	.00
10	A2	0	366.33	-8.31	30.11	7.61	336.93	.00	.00	64	A2	0	225.07	-62.73	-69.84	9.23	348.66	.00	.25
	B20	0		-9.45	37.91	1.73	336.17	.00	.02		B20	0		-55.70	-71.20	1.42	350.78	.00	.23
	B2	1		-9.37	37.85	1.71	336.16	.00	.02		B2	2		-53.08	-73.46	1.39	350.47	.00	.24
	C2	4		-9.37	37.85	1.69	336.16	.00	.00		C2	4		-53.18	-73.73	1.55	350.43	.00	.00
18	A2	0	366.33	-8.82	10.32	17.24	347.59	.00	.00	72	A2	0	225.07	-82.28	-70.95	35.90	342.52	.00	.11
	B20	0		-7.00	23.21	1.64	348.48	.00	.00		B20	0		-60.95	-61.54	1.58	346.00	.00	.07
	B2	1		-6.83	23.07	1.63	348.46	.00	.00		B2	2		-60.30	-62.11	1.44	345.92	.00	.07
	C2	4		-6.83	23.09	1.61	348.46	.00	.00		C2	2		-60.37	-62.20	1.73	345.91	.00	.00
19	A2	0	698.99	87.72	148.78	83.55	379.90	.00	.97	73	A2	0	216.53	-87.65	-74.53	37.75	341.08	.00	.11
	B20	0		96.86	214.89	5.09	383.24	.00	1.09		B20	0		-64.25	-65.36	1.58	344.63	.00	.07
	B2	2		98.65	213.33	5.07	383.01	.00	1.08		B2	1		-63.67	-65.87	1.58	344.56	.00	.07
	C2	5		98.23	212.55	5.31	382.89	.00	.01		C2	2		-63.74	-65.95	1.67	344.55	.00	.00
27	A2	0	698.99	53.53	69.95	176.27	399.49	.00	.26	81	A2	0	216.53	-86.35	-98.66	68.61	333.01	.00	.07
	B20	0		105.72	172.61	8.94	412.44	.00	.73		B20	0		-37.79	-85.36	1.90	337.80	.00	.01
	B2	2		109.27	169.63	8.81	411.98	.00	.71		B2	1		-36.88	-86.17	1.90	337.70	.00	.00
	C2	6		108.89	169.09	9.11	411.89	.00	.00		C2	3		-36.92	-86.19	1.96	337.69	.00	.00
28	A2	0	654.11	37.09	48.46	170.42	398.28	.00	.15	82	A2	0	347.06	-21.74	-74.10	105.50	337.42	.00	.00
	B20	0		90.36	144.46	8.67	411.14	.00	.53		B20	0		43.18	-42.48	2.43	343.94	.00	.04
	B2	2		93.08	142.19	8.57	410.78	.00	.51		B2	1		42.81	-42.16	2.44	343.98	.00	.04
	C2	6		92.75	141.73	8.92	410.71	.00	.00		C2	3		42.76	-42.20	2.48	343.98	.00	.00
36	A2	0	654.11	54.53	56.70	125.96	417.10	.00	.19	90	A2	0	347.06	-11.26	-84.69	105.25	337.77	.00	.00
	B20	0		69.67	88.44	76.15	420.07	.00	.22		B20	0		47.69	-49.01	3.15	345.31	.00	.07
	B2	2		70.61	86.96	76.91	419.84	.00	.21		B2	2		46.99	-48.41	3.17	345.39	.00	.07
	C2	6		71.92	88.39	73.73	420.07	.00	.00		C2	4		46.92	-48.47	3.23	345.38	.00	.00
37	A2	0	262.56	-99.93	-83.21	57.84	388.11	.00	.25	91	A2	0	696.15	121.11	16.19	203.07	356.15	.00	.35
	B20	0		-84.34	-86.20	42.10	391.22	.00	.21		B20	0		213.54	109.88	5.16	368.51	.00	.93
	B2	2		-82.58	-87.13	41.41	391.08	.00	.21		B2	2		217.53	106.44	5.07	368.01	.00	.90
	C2	4		-83.69	-88.72	44.13	390.84	.00	.00		C2	5		216.99	105.98	5.23	367.95	.00	.00
45	A2	0	262.56	-54.21	-86.38	32.78	370.59	.00	.21	99	A2	0	696.15	114.75	28.68	190.02	363.29	.00	.59
	B20	0		-39.84	-76.32	3.36	375.50	.00	.13		B20	0		183.48	131.02	6.36	376.66	.00	1.37
	B2	2		-38.18	-77.74	3.33	375.29	.00	.14		B2	2		190.08	125.33	6.23	375.83	.00	1.31
	C2	5		-38.26	-77.94	3.50	375.26	.00	.00		C2	5		189.41	124.56	6.46	375.72	.00	.01
46	A2	0	250.21	-54.58	-89.22	26.05	368.21	.00	.24	100	A2	0	626.69	87.46	10.28	169.23	360.13	.00	.41
	B20	0		-42.26	-82.99	3.00	372.62	.00	.17		B20	0		147.61	101.57	6.00	372.54	.00	1.04
	B2	2		-40.16	-84.78	2.97	372.36	.00	.18		B2	2		153.15	96.79	5.90	371.85	.00	.99
	C2	5		-40.24	-85.02	3.14	372.32	.00	.00		C2	5		152.66	96.19	6.08	371.76	.00	.01

Table 15. Same as in Table 14, Except for Gridpoint (7,4)

Gridpoint (7,4)										Gridpoint (7,4)									
ns	model	m	FD	H	G	E	FU	S	B	ns	model	m	FD	H	G	E	FU	S	B
1	A2	0	375.53	45.44	14.39	-85.44	401.22	.00	.08	100	A2	0	547.50	9.90	2.89	114.55	420.22	.00	.05
	B20	0		41.73	21.89	-89.00	400.93	.62	.03		B20	0		7.20	-1.21	121.81	419.71	.00	.01
	B2	1		41.86	21.92	-89.15	400.93	.00	.03		B2	3		6.68	-4.04	125.33	419.55	.00	.01
	C2	3		40.48	20.62	-86.38	400.81	.00	.00		C1	3		7.02	-2.97	123.84	419.61	.00	.00
10	A2	0	566.12	23.25	34.66	97.56	407.74	.00	-2.92	109	A2	0	372.13	-14.22	-56.35	31.16	411.54	.00	.01
	B20	0		24.45	63.89	66.84	407.91	3.07	.03		B20	0		-12.03	-73.44	45.55	412.05	.00	.00
	B2	2		23.77	60.52	71.18	407.71	2.96	.03		B2	1		-11.96	-73.38	45.42	412.05	.00	.00
	C2	4		24.09	61.22	70.08	407.75	2.98	.00		C2	2		-11.89	-73.10	45.06	412.07	.00	.00
19	A2	0	649.78	30.59	49.68	152.02	417.00	.00	-.48	118	A2	0	338.69	-14.88	-47.61	-2.60	403.76	.00	.01
	B20	0		31.85	105.78	94.82	417.19	.59	.05		B20	0		-13.28	-57.16	4.89	404.23	.00	.00
	B2	2		30.98	98.44	102.91	416.92	.57	.04		B2	1		-13.05	-57.28	4.79	404.23	.00	.00
	C2	4		31.66	100.93	99.60	417.01	.57	.00		C2	3		-13.04	-57.25	4.75	404.23	.00	.00
28	A2	0	510.34	11.03	-2.88	80.53	418.61	.00	-3.05	127	A2	0	339.87	-14.98	-24.38	-23.58	402.80	.00	.01
	B20	0		13.49	21.17	53.28	419.02	3.39	.02		B20	0		-16.11	-33.19	-13.32	402.49	.00	.00
	B2	2		12.98	16.98	58.22	418.89	3.30	.02		B2	1		-15.86	-33.53	-13.21	402.80	.00	.01
	C2	3		13.37	18.92	55.76	418.95	3.34	.00		C2	3		-15.91	-33.44	-13.26	402.48	.00	.00
37	A2	0	412.47	-11.71	-23.94	30.47	417.39	.00	-.26	136	A2	0	338.79	-15.79	-26.69	-21.49	402.75	.00	.01
	B20	0		-10.01	-22.22	26.67	417.65	.37	.00		B20	0		-16.74	-36.34	-10.61	402.49	.00	.01
	B2	1		-10.36	-23.77	28.66	417.60	.35	.00		B2	1		-16.43	-36.72	-10.52	402.46	.00	.01
	C2	1		-10.05	-22.35	26.85	417.65	.37	.00		C1	1		-16.47	-36.64	-10.56	402.47	.00	.00
46	A2	0	411.23	-15.68	-13.98	24.91	416.07	.00	.09	145	A2	0	346.91	-13.47	-30.71	-9.35	400.43	.00	.00
	B20	0		-15.05	-9.81	19.97	416.17	-.07	.00		B20	0		-13.43	-37.52	-2.58	400.44	.00	.00
	B2	1		-15.31	-10.93	21.42	416.13	-.08	.00		B2	1		-13.27	-37.64	-2.60	400.43	.00	.00
	C2	1		-15.06	-9.78	19.96	416.17	-.07	.00		C2	3		-13.27	-37.59	-2.66	400.43	.00	.00
55	A2	0	403.12	-19.17	-18.30	25.52	415.12	.00	.04	154	A2	0	720.97	80.16	106.99	170.72	413.29	.00	.19
	B20	0		-17.98	-16.69	22.53	415.28	-.02	.00		B20	0		70.45	141.84	97.11	411.62	.15	.20
	B2	1		-18.30	-17.75	23.95	415.23	-.03	.00		B2	1		72.18	138.88	98.53	411.42	.15	.20
	C2	1		-17.99	-16.66	22.51	415.28	-.02	.00		C2	1		71.35	136.81	101.38	411.29	.15	.01
64	A2	0	393.24	-19.82	-21.50	21.56	413.01	.00	.00	163	A2	0	897.32	141.83	72.36	268.05	414.59	.00	-.49
	B20	0		-18.22	-21.74	19.99	413.20	.00	.00		B20	0		174.80	176.61	136.37	418.91	1.15	.53
	B2	1		-18.50	-22.48	21.05	413.17	.00	.00		B2	2		179.34	170.71	128.14	418.51	1.14	.52
	C2	1		-18.22	-21.75	20.01	413.20	.00	.00		C2	5		178.48	169.22	130.08	418.41	1.13	.00
73	A2	0	368.91	-12.72	-26.37	-3.16	411.15	.00	-.01	172	A2	0	572.21	51.17	-53.20	172.29	402.05	.00	.10
	B20	0		-11.95	-31.49	1.09	411.24	.01	.00		B20	0		104.96	19.31	40.01	408.11	.00	.18
	B2	1		-11.95	-31.52	1.12	411.24	.01	.00		B2	2		107.65	16.95	39.83	407.95	.00	.18
	C2	1		-11.98	-31.60	1.24	411.24	.01	.00		C2	4		107.48	16.68	40.12	407.93	.00	.01
82	A2	0	666.72	38.66	49.34	162.61	415.83	.00	-.28	181	A2	0	282.15	-72.56	-141.16	112.53	383.35	.00	.01
	B20	0		44.33	100.08	105.31	416.65	.43	.07		B20	0		-15.50	-104.78	13.13	389.31	.00	.00
	B2	2		43.68	93.64	112.75	416.30	.41	.06		B2	1		-15.53	-104.76	13.13	389.31	.00	.00
	C2	4		43.91	94.21	111.85	416.33	.41	.00		C2	2		-15.60	-104.88	13.33	389.30	.41	.00
91	A2	0	713.55	34.92	51.95	205.43	421.35	.00	.10	190	A2	0	265.18	-61.87	-113.08	70.06	370.08	.00	.01
	B20	0		34.72	85.80	171.74	421.34	.00	.05		B20	0		-28.59	-89.12	8.92	373.98	.00	.00
	B2	2		34.70	81.66	176.12	421.12	.00	.05		B2	1		-28.57	-89.15	8.92	373.98	.00	.00
	C2	4		33.93	79.77	178.84	421.02	.00	.00		C2	3		-28.60	-89.22	9.03	373.97	.00	.00

the most accurate of all.

5. SUMMARY AND CONCLUSIONS

We analyzed the changes in formula recommended by the OSU group and assessed their effects on the energy exchanges between the atmosphere and its underlying earth. We also described in detail the rationale of the new procedure of evaluating the surface variables that balance energy fluxes and considered different levels of approximation in solving the balance equations. We then utilized GCM-generated atmospheric conditions to carry out static tests on impacts of the changes on the surface outputs over land in wintertime.

The results of tests confirmed our earlier notion that the modifications have only minor influences on surface temperature and humidity in the sense that resulting changes are small in comparison with their responses to synoptic conditions. Their impacts on individual surface energy fluxes are, however, significantly greater and likely to produce changes in the dynamics of the atmosphere with time.

The new formulas for surface-layer exchange coefficients were found to yield greater diurnal amplitudes without affecting their phases in both temperature and specific humidity at the surface, in response to reduced efficiencies of the surface exchanges. The change is generally larger in the day than at night. As a result, on a typical day where the diurnal cycle is well defined, the change in formulas brought higher daily means and greater daily standard deviations. The corresponding changes in fluxes are best seen in smaller values of the daily standard deviations of sensible-heat and evaporative latent-heat fluxes. Daily mean values of these fluxes are, on the other hand, of little value in representing this characteristic, because balanced values of the individual fluxes are affected by other aspects of the environment.

The response of the model to the change in algorithm was found to be rather different from that described above. We found, first of all, difference between the east and the west. In the west, where large diurnal amplitudes in surface temperature characterized the study period, the new algorithm yielded higher surface temperature

and drier surface humidity, accompanied by more positive sensible heat flux but smaller evaporative latent heat flux. The differences in magnitude of the fluxes were as great as those due to the change in the formulas for the exchange coefficients. In the east, where rain and overcast weather prevailed most of the period and dampened the diurnal amplitudes, there was little difference in most of the surface outputs. The limited size of samples of this study precludes us from determining whether the climatic or synoptic conditions were responsible for this contrast.

The investigation into the method of solving the energy balance equation showed that even though there are differences in the values of the outputs due to the difference in method, those differences are generally much smaller than the differences due to the change either in the formulas or in the algorithm. Within the currently achievable accuracy on the individual flux values, we believe the non-iterative method applied to the linearized balance equations can provide an adequate estimate of the surface outputs.

Finally, we recommend that all the proposed changes be incorporated into the PL-GSM for global runs and that the results be subjected to analysis over wider regions for the dynamic effects in the global context.

References

1. Brenner, S., Yang, C., and Yee, S. (1982) *The AFGL Spectral Model of the Moist Global Atmosphere: Documentation of the Baseline Version*, AFGL-TR-83-0393, Air Force Geophysics Laboratory, Hanscom AFB, MA, AD129283.
2. Brenner, S., Yang, C., and Mitchell, K. (1984) *The AFGL Global Spectral Model: Expanded Resolution Baseline Version*, AFGL-TR-84-0308, Air Force Geophysics Laboratory, Hanscom AFB, MA, ADA160370.
3. Yang, C., Mitchell, K., Norquist, D., and Yee, S. *Diagnostics for and Evaluation of New Physical Parameterization Schemes for Global NWP Models*, GL-TR-89-0158, Geophysics Laboratory (AFSC), Hanscom AFB, MA. ADA228033.
4. Norquist, D., Yang, C., Chang, S. and Hahn, D. (1992) *Phillips Laboratory Global Spectral Numerical Weather Prediction Model*, PL-TR-92-2225, Phillips Laboratory, Hanscom AFB, MA, 154 pp. ADA267293,
5. Mahrt, L., Pan, H.-L., Paumier, J., and Troen, Ib (1984) *A Boundary Layer Parameterization for a General Circulation Model*, AFGL-TR-84-0063, ADA144224, Air Force Geophysics Laboratory, Hanscom AFB, MA.
6. Mahrt, L., Pan, H.-L., Ruscher, P., and Chu, C.-T. (1987) *Boundary Layer Parameterization for a Global Spectral Model*, AFGL-TR-87-0246, ADA199440, Air Force Geophysics Laboratory, Hanscom AFB, MA.
7. Ek, M. and Mahrt, L. (1991) *OSU 1-D PBL Model User's Guide Version 1.0.4*, Department of Atmospheric Sciences, Oregon State University, Corvallis, OR.

8. Mahrt, L., Ek, M., Sun, J., and French, M. (1994) *Marine Boundary-Layer Parameterizations for Large-Scale Models*, PL-TR-94-2128, ADA282402, Phillips Laboratory, Directorate of Geophysics, Hanscom AFB, MA.
9. Miller, M.J., Beljaars, A.C.M., and Palmer, T.N. (1992) The Sensitivity of ECMWF Model to the Parameterization of Evaporation from the Tropical Oceans, *J. Climate*, **5**, pp. 418-434.
10. Holtslag, A.A.M. and Beljaars, A.C.M. (1988) Surface Flux Parameterization Schemes: Developments and Experiences at KNMI, Parameterization of Fluxes over Land Surfaces, Workshop Proceedings, October 1988, ECMWF, Reading, England, pp. 121-147.
11. Charnock, H. (1955) Wind Stress on a Water Surface, *Quart. J. Roy Meteorol. Soc.*, **81**, pp. 639-640.
12. Smith, S. (1980) Wind Stress and Heat Flux over the Ocean in Gale Force Winds, *J. Phys. Oceanogr.*, **10**, pp. 709-726.
13. SethRaman, S. and Raynor, G.S. (1975) Surface Drag Coefficients Dependence on the Aerodynamic Roughness of the Sea, *JGR*, **80**, pp. 4983-4988.
14. Monteith, J.L. (1965) Evaporation and Environment, *Symposia Soc. Exp. Biol.*, **19**, pp. 206-234.
15. Brunt, D. (1939) *Physical and Dynamical Meteorology*, Cambridge University Press.
16. Penman, H.L. (1963) *Vegetation and Hydrology*, Tech. Comm. 53, Commonwealth Bur. of Soils, Harpenden, England.